

Series 02 Flight Mechanics 03

Optimum Cruise Performance of Subsonic Transport Aircraft

E. Torenbeek



Delft University Press



706389

Optimum Cruise Performance of Subsonic Transport Aircraft

Bibliotheek TU Delft



C 3021896

Series 02: Flight Mechanics

03



Optimum Cruise Performance of Subsonic Transport Aircraft

E. Torenbeek



Delft University Press / 1998

2392
330
2

Published and distributed by:

Delft University Press
Mekelweg 4
2628 CD Delft
The Netherlands
Telephone +31 (0)15 278 32 54
Fax +31 (0)15 278 16 61
e-mail: DUP@DUP.TUDelft.NL

by order of:

Faculty of Aerospace Engineering
Delft University of Technology
Kluyverweg 1
P.O. Box 5058
2600 GB Delft
The Netherlands
Telephone +31 (0)15 278 14 55
Fax +31 (0)15 278 18 22
e-mail: Secretariaat@LR.TUDelft.NL
website: <http://www.lr.tudelft.nl/>



*Cover: Aerospace Design Studio, 66.5 x 45.5 cm, by:
Fer Hakkart, Dullenbakkersteeg 3, 2312 HP Leiden, The Netherlands
Tel. +31 (0)71 512 67 25*

90-407-1579-3

Copyright © 1998 by Faculty of Aerospace Engineering

All rights reserved.

No part of the material protected by this copyright notice may be reproduced or utilized in any form or by any means, electronic or mechanical, including photocopying, recording or by any information storage and retrieval system, without written permission from the publisher: Delft University Press.

Printed in The Netherlands

Contents

1	Cruise Performance for Preliminary Design	1
1.1	Types of Performance Problems	1
1.2	Optimum Cruise Performance	2
1.3	Scope of this Report	3
2	The Ratio of Lift to Drag	5
2.1	Partial and Unconstrained Optima	9
2.2	Constraints on Altitude or Thrust	13
3	The Parameter ML/D	15
3.1	Maximum ML/D at Subcritical Speeds	16
3.2	ML/D with Compressibility Effects	18
4	The Specific Range	21
4.1	Generalized Engine Performance	22
4.2	Maximum range parameter	23
4.3	Interpretation of the Derivative η_M	28
4.4	Refinements in the Optima	31
5	Analysis of Cruising Flight	34
5.1	The Generalized Range Equation	34
5.2	Range at Subcritical Speeds	35
5.3	Range at High Speeds	38
6	Prediction of the Fuel Load	41
6.1	Mission Fuel	44
6.2	Reserve and Total Fuel	46
7	Summary of Results	49
A	Statistical Derivation of the Range Parameter	53
	Bibliography	58

NOMENCLATURE

a	= speed of sound	(m/s)
C_D	= drag coefficient	(-)
$C_{D,0}$	= zero-lift drag coefficient	(-)
C_D^*	= minimum drag coefficient	(-)
C_{D_L}	= logarithmic derivative of C_D w.r.t. C_L	(-)
C_{D_M}	= logarithmic derivative of C_D w.r.t. M	(-)
C_L	= lift coefficient	(-)
C_L^*	= lift coefficient for minimum drag coefficient	(-)
C_P	= Power Specific Fuel Consumption	((N/s)/ W)
C_T	= Thrust Specific Fuel Consumption	((N/s)/ N)
D	= drag	(N)
F	= fuel weight flow per unit time	(N/s)
f_1, f_2, f_3, f_4	= generalized engine performance functions	(-)
g	= acceleration due to gravity	(m/s^2)
H	= calorific value of jet engine fuel	(J/kg)
h	= altitude	(m)
h_e	= energy height	(m)
K	= induced drag factor	(-)
k_R	= factor accounting for flight schedule	(-)
k_{res}	= reserve fuel fraction	(-)
L	= lift	(N)
M	= Mach number	(-)
\dot{m}	= mass flow per unit time	(kg/s)
N	= engine RPM	(-)
n	= exponent of M in approximation for TSFC	(-)
\mathcal{P}	= Range Parameter	(-)
P_{br}	= engine shaft power	(W)
p	= atmospheric pressure	(N/m^2)
q	= dynamic pressure	(N/m^2)
R	= range, distance flown	(m)
\mathcal{R}	= equivalent all-out range in cruising flight	(m)
R_H	= range-equivalence of fuel calorific value, $R_H = H/g$	(m)
R_h	= harmonic or nominal range	(m)
S	= reference wing area	(m^2)
\mathcal{SR}	= Specific Range	(m/N)
T	= net Thrust	(N)
t	= time	(s)
V	= true airspeed	(m/s)
v_j	= mean exhaust jet velocity	(m/s)
W	= weight (no index: All Up Weight)	(N)
y	= $C_L/C_{L,md}$	(-)

γ	= ratio of specific heats of air, $\gamma = 1.40$	(-)
Δ	= increment	(-)
δ	= relative ambient pressure	(-)
ζ	= fuel weight fraction	(-)
η	= overall powerplant efficiency	(-)
η_{prop}	= propeller efficiency	(-)
η_M	= logarithmic derivative of η w.r.t. Mach number	(-)
η_T	= logarithmic derivative of η w.r.t. T/δ	(-)
θ	= relative ambient temperature	(-)
ρ	= atmospheric density	(kg/m^3)
Φ	= normalized slope of payload range diagram	(-)

Indices

cb	= combustion
cl	= climb
ctg	= contingency
cr	= cruise
dd	= drag divergence
div	= diversion
eq	= equivalent
F	= fuel
f	= end of cruising
h, es	= horizontal flight, constant engine setting
h, l	= horizontal cruise, constant lift coefficient
h, M	= horizontal flight, constant Mach number
$hold$	= holding
i	= initial cruising
$land$	= landing
m	= mission
max	= maximum
md	= minimum drag for constant M
opt	= optimum
p	= payload
pr	= propulsion
$prop$	= propeller
res	= reserve fuel
sl	= Sea Level, ISA
th	= thermal
to	= take-off

Abbreviations

ATC	= Air Traffic Control
AUW	= All Up Weight
BSFC	= Brake Specific Fuel Consumption
DOC	= Direct Operating Cost
EAS	= Equivalent Air Speed
EGT	= Exhaust Gas Temperature
ESDU	= Engineering Sciences Data Unit
GA	= General Aviation
HSC	= High Speed Cruise
ISA	= International Standard Atmosphere
LRC	= Long Range Cruise
LW	= Landing Weight
MTOW	= Maximum Take Off Weight
MZFW	= Maximum Zero Fuel Weight
OEW	= Operating Empty Weight
RPM	= Revolutions Per Minute
SL	= Sea Level
SR	= Specific Range
SST	= Super-Sonic Transport
TC	= Transport Category
TIT	= Turbine Inlet Temperature
TSFC	= Thrust Specific Fuel Consumption
TOW	= Take Off Weight
UL	= Useful Load
ZFW	= Zero Fuel Weight



Chapter 1

Cruise Performance for Preliminary Design

1.1 Types of Performance Problems

During the design process of Transport Category (TC) and General Aviation (GA) aircraft the designer(s) will inevitably be confronted with at least one of the following questions:

- What are, for a given aircraft/engine combination, the best cruise altitude and speed from the point of view of minimum fuel consumed per unit time elapsed or per distance travelled ?
- For a specified flight mission, how to estimate the (minimum) amount of fuel and time required? In addition to cruise fuel and time this problem involves an estimation of the fuel quantities required for the other phases of the flight, in particular climb and descent, and reserve fuel estimation.
- How to find the best operational flight profile of a transport aircraft, resulting in minimum fuel consumed, elapsed time or Direct Operating Costs (DOC) with or without constraints on range or time travelled.

From the flight mechanical point of view all three questions are closely related to the generalized problem of trajectory optimization. The *first problem* is the most basic and is usually treated as an instantaneous performance¹ problem, assuming equilibrium of forces in horizontal flight: Lift = Weight and Thrust = Drag. The *second problem* is more complicated since it involves integration of the instantaneous performance into path performance. Moreover, the Take Off Weight (TOW) is an input to the computation of the fuel load, but it is also an outcome of this calculation in case the Zero Fuel Weight (ZFW) is specified. Practical numerical procedures exist to solve this problem—for example the Newton-Raphson approach—but for preliminary design it would be nice to avail of a

¹Also referred to as “point performance”.

closed-form solution. The cruise sector is usually treated as a (quasi) steady flight, with either constant or very gradual variations of the altitude and/or the speed.

The *third problem* is by far the most complicated from the mathematical and numerical points of view, since the flight mechanics involved have to be treated as a dynamic problem and the optimization requires the calculus of variations or optimal control theory. Applications are mostly found in the operational use, with the objective of achieving fuel reductions or devising optimum Air Traffic Control (ATC) procedures. Since fuel savings obtained appear to be very modest—at least for medium and long range flights—it is not common practice to use this compute-intensive technique in the preliminary design stage. The optimal trajectory analysis forms a subject in itself, which is not treated in the present report; for a review the reader is referred to Visser [29].

1.2 Optimum Cruise Performance

This Report treats the computation of range and fuel required for high speed commercial aircraft. Cruise performance of propeller aircraft is a classical problem which is adequately covered in the literature, hence it will not be treated explicitly, although the generalized method presented applies to propeller aircraft as well. Moreover the optimization of endurance or flight time is excluded from the analysis; the emphasis is on maximum range or minimum fuel. Flight conditions for minimum Direct Operating Costs (DOC) will not be considered primarily because the results are quite specific to the operational environment. Two more subjects are excluded from the analysis:

- the effects of wind on cruise performance are disregarded; for a concise treatment see Hale (1979) [10];
- Super-Sonic Transports (SST's) are not considered explicitly, although the approach developed is applicable to this aircraft category, provided one is aware of the existence of dual optima at subsonic and supersonic speeds.

This leaves us with the cruise performance problem of high subsonic jet aircraft which fly most effectively at high altitudes, unless ATC requirements or non-standard conditions—for example engine failure—impose a limit on speed or altitude.

The question is justified as to whether the problem of cruise performance needs to be considered any more after so many years of successful operation of commercial aircraft. The subject is also treated extensively in several modern textbooks; see for example Shevell [24], Mair and Birdsall [12] and Ruijgrok [21]. However, there remain several misunderstandings and questions to be answered about range performance as illustrated by the following brief review of the literature.

The first analyses of range for turbojet powered aircraft were published soon after WWII, in the UK by Page [18] and Edwards [8], and in the US by Jonas [11], Ashkenas [4], and Perkins and Hage [20]. The range equations were based either on a cruise/climb technique with constant speed and lift coefficient—resulting in the Bréguet equation for jet

propulsion—or on horizontal flight with constant lift coefficient, resulting in the “square-root” equation [11]. Although the cruise/climb technique results in longer ranges than horizontal cruising flight, it is usually not a favoured operational procedure due to ATC-imposed constraints. But the alternative cruise technique leads to decreasing airspeed and thrust settings as fuel is consumed during the flight—which is not practical either—and inferior range performance. Alternative procedures were developed later [19] for horizontal cruising flight at constant speed, Mach number or engine rating. They are summarized in various ESDU Data Items, [2] and [3].

There is agreement in the literature as to the fact that—for specified initial altitude and speed—a cruise/climb flight program yields the longest range. There is, however, no consensus about the definition of the best initial or mean altitude and speed. In particular the ratio of optimum flight speed to the Minimum Drag Speed has been debated by several authors, even in recent publications. For example, Hale (1976)[9] points out that different values have been derived for this ratio—namely $2^{1/4}$ and $3^{1/4}$, dependent on cruise technique—and concludes from analysis that the latter value is the correct one. Ironically, his derivation presupposes an implicit altitude constraint which inevitably leads to the following question: which altitude is the best if the constraint is deleted? Bert [6] derived a “new range equation”, in fact a modification of the “arctan range equation” for flight at constant altitude and speed that can be found already in Edwards’ work [8]. He computed in an example an optimum speed equal to 1.864 times the speed for minimum drag—an unusual result, caused by a continuously decreasing Thrust Specific Fuel Consumption (TSFC) with increasing speed. In a recent article Miller [13] concludes that the best altitude is one where the drag is a global minimum, “which disproves the theory that the cruise lift/drag ratio is $\sqrt{3}/2$ times the maximum lift/drag ratio”, corresponding to a flight speed equal to $3^{1/4}$ times the Minimum Drag Speed.

1.3 Scope of this Report

Most of the conflicting results from the literature must be ascribed to the fact that below the drag rise there is no unconstrained optimum flight condition for maximum range, as will be shown by the present analysis. Early publications—for example by Page [18]—point out by means of examples that optimum cruise Mach numbers might occur in the drag rise. To the best knowledge of the author the first derivation of an analytical criterion for optimum flight Mach number has been given by Backhaus [5]. Miele [17] wrote a thorough treatment of optimum cruise performance at transonic speeds, but practical applications of his rather complex theory have not been found in the literature. The generalized criteria for maximum Specific Range derived by Torenbeek and Wittenberg [27]—which are valid at high subsonic speeds and for arbitrary propulsion systems—have been referred to as “fairly sophisticated” by Martinez-Val et al [15]. Since they provide the basis for a comprehensive theoretical fundament, these criteria will be readdressed in the present Report and further augmented to derive range performance and stage fuel required.

In the first chapters the effects of compressibility on the lift/drag ratio and on the specific range will be treated. Conditions will be derived for the best flight Mach number and cruise altitude resulting in maximum range of aircraft with various types of gas turbine based propulsion systems: turboprops, turbojets and turbofans. Analytical conditions will be derived for the unconstrained optimum lift coefficient and Mach number, as well as for the case of constraints on the altitude or the engine thrust. The second part deals with the problem of making a good estimate of the fuel required during the cruising flight and of the total fuel required to fly a specified mission, including reserves. The complication that flight takes place at transonic speeds makes it necessary to reconsider the flight techniques for optimum range performance and minimum stage fuel required. Finally a useful method will be selected on the basis of accuracy, simplicity and suitability to preliminary aircraft design optimization studies, which require knowledge of the sensitivity of the fuel load to variations in the aircraft design characteristics.

Chapter 2

The Ratio of Lift to Drag

The lift/drag ratio—sometimes referred to as the aerodynamic fineness ratio or aerodynamic efficiency—is an important performance parameter, since it determines the drag and thrust required in horizontal flight,

$$T = D = \frac{W}{L/D} \quad (2.1)$$

For given Specific Fuel Consumption of the powerplant, the fuel flow rate is therefore inversely proportional to the lift/drag ratio, which is determining to a large extent:

- the endurance and range for a given amount of fuel,
- the amount of fuel required to fly during a specified time period or to cover a specified distance.

The aircraft drag coefficient of high speed transport aircraft,

$$C_D = \frac{D}{qS} \quad (2.2)$$

is a function of the lift coefficient

$$C_L = \frac{L}{qS} \quad (2.3)$$

and the flight Mach number

$$M = V/a \quad (2.4)$$

where the dynamic pressure is defined as

$$q = 1/2\rho V^2 = 1/2\gamma p M^2 \quad (2.5)$$

Most aircraft with low subsonic speeds feature a single drag polar for the en route configuration, independent of the Mach number:

$$C_D = C_D(C_L) \quad (2.6)$$

Although variations of Reynolds number and center of gravity location theoretically have an effect on the drag polar, this is usually ignored in preliminary design and drag polars are referred to mean conditions of loading and typical flight profiles. Some aircraft feature a slight variation of the drag coefficient with Mach number at low subsonic speeds, mainly due to variation in Reynolds number. Compressibility effects come into play at high subsonic speeds, and the drag coefficient has to be expressed in terms of the lift coefficient and Mach number

$$C_D = C_D(C_L, M) \quad (2.7)$$

A representative set of drag polars is depicted on Figure 2.1a; an alternative representation of the same data is presented in Figure 2.1b. For the example aircraft there is a gradual drag reduction with Mach number at low speeds, which may be caused by an increasing Reynolds number and/or decreasing skin friction associated with the heating up of the boundary layer. For low lift coefficients the drag begins to increase first in the form of a “drag creep” for Mach numbers in excess of about 0.65, while for lift coefficients in excess of 0.50 there is also a Mach number effect at low speeds. This drag increase is probably caused by compressibility effects at locations where pressure peaks occur, e.g. at the nose of the airfoils. For Mach numbers above ≈ 0.80 the drag rise is much faster: the so-called “drag divergence”. The usual definition of the drag divergence Mach number M_{dd} is based on the slope of the drag curve for constant lift coefficient,

$$\frac{\partial C_D}{\partial M} = 0.10 \quad (2.8)$$

This condition defines a Mach number which depends on the lift coefficient and therefore the drag initiation is represented in the figure by a curve. By using these drag polars, values of the lift/drag ratio have been derived—see Figure 2.2a—and contours of constant L/D ratios have been plotted on Figure 2.2b. These contour plots have the advantage that constant L/D curves do not intersect since each combination of the independent variables C_L and M define only one drag coefficient. This drag representation is therefore completely unambiguous.

The thrust required in horizontal steady flight follows directly from Equation 2.1

$$T = D = \frac{W}{C_L/C_D} \quad (2.9)$$

The condition for maximum lift/drag *for given Mach number*—resulting in minimum drag (md) and hence minimum thrust—is defined by the lift coefficient $C_{L,md}$.

For low subsonic aircraft designed to cruise at speeds up to about $M \approx 0.6$, the lift coefficient $C_{L,md}$ has a unique value defining the Minimum Drag Speed, which is obtained from Equation 2.3, with $L = W$:

$$V_{md} = \sqrt{\frac{2W/S}{\rho C_{L,md}}} \quad (2.10)$$

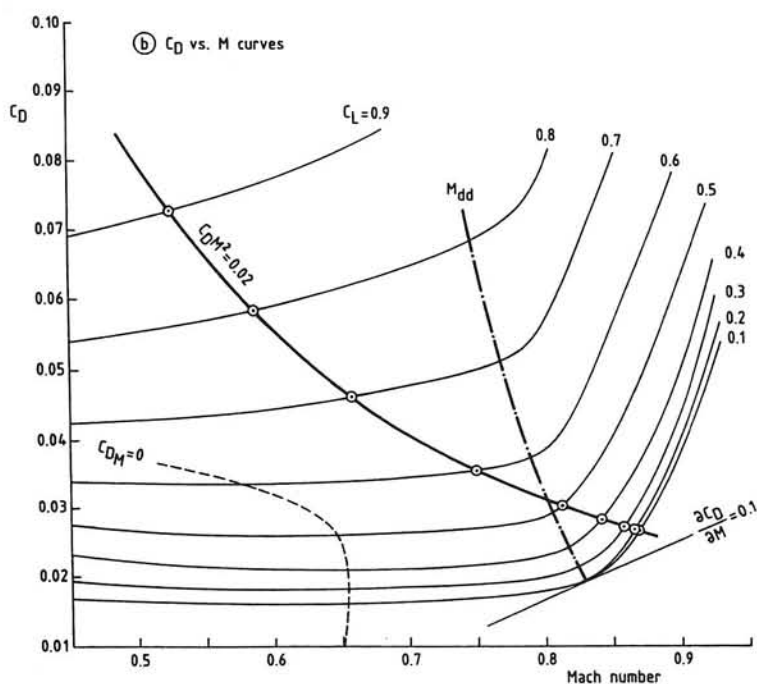
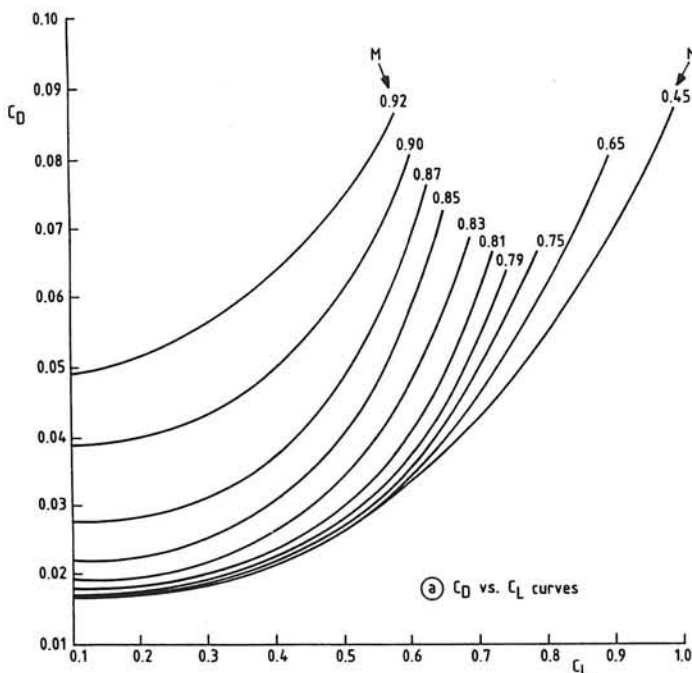


Figure 2.1: Drag polars of a high subsonic transport aircraft

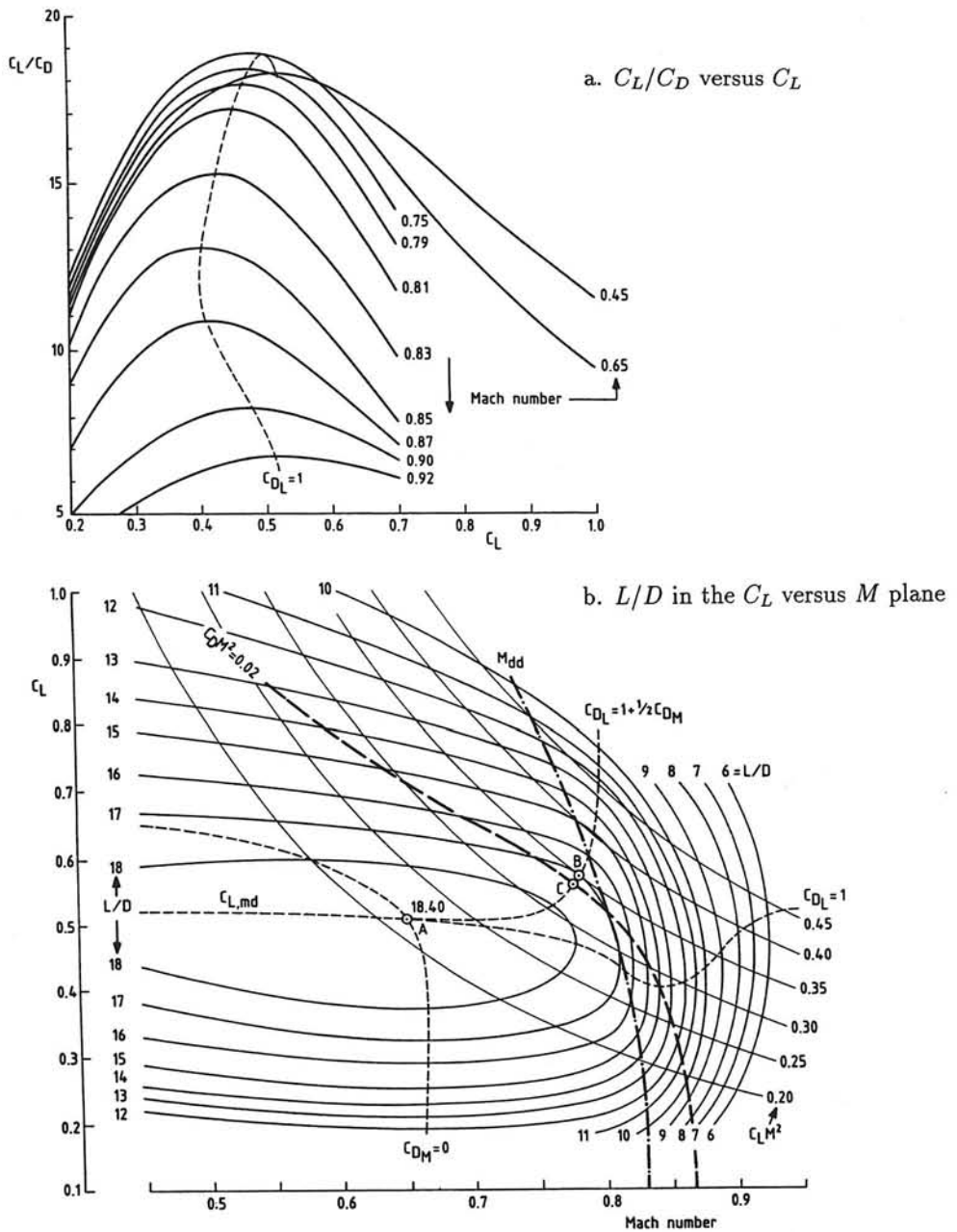


Figure 2.2: Different representations of the lift to drag ratio

or the Mach number¹:

$$M_{md} = \sqrt{\frac{2W/S}{\gamma p C_{L,md}}} \quad (2.11)$$

In this case the Minimum Drag Speed is thus a constant Equivalent Air Speed (EAS), provided the All Up Weight (AUW) is specified.

For high subsonic aircraft $C_{L,md}$ is a function of the Mach number; the example in Figure 2.2b indicates that it is nearly constant for Mach numbers up to about 0.65. Above this speed the effects of compressibility on drag result in rapidly decreasing values of the L/D ratio. The contours of constant L/D values are almost straight at low speeds but become closed at high Mach numbers, and a dip occurs in $C_{L,md}$ at high Mach numbers.

2.1 Partial and Unconstrained Optima

The mathematical condition of maximum L/D is—for the case of general drag polars according to Equation 2.7—obtained from logarithmic differentiation:

$$d \log(C_L/C_D) = d \log C_L - d \log C_D = 0 \quad (2.12)$$

with

$$d \log C_D = \frac{\partial \log C_D}{\partial \log C_L} d \log C_L + \frac{\partial \log C_D}{\partial \log M} d \log M \quad (2.13)$$

The following logarithmic derivatives are now introduced,

$$C_{D_L} \stackrel{\text{def}}{=} \frac{\partial \log C_D}{\partial \log C_L} = \frac{C_L}{C_D} \frac{\partial C_D}{\partial C_L} \quad (\text{constant } M) \quad (2.14)$$

$$C_{D_M} \stackrel{\text{def}}{=} \frac{\partial \log C_D}{\partial \log M} = \frac{M}{C_D} \frac{\partial C_D}{\partial M} \quad (\text{constant } C_L) \quad (2.15)$$

From their definitions it is clear that logarithmic derivatives can be interpreted as a percentage change in a dependent variable due to a given percentage change of the independent variable. Log-derivatives are therefore non-dimensional; their numerical value is often between zero and plus or minus two or three, which is convenient for numerical treatment.

After substitution of the log-derivatives Equation 2.13 reads as follows,

$$d \log C_D = C_{D_L} d \log C_L + C_{D_M} d \log M \quad (2.16)$$

¹In the case of a constraint on the thrust the Mach number for minimum drag is obtained from the equilibrium Thrust=Drag.

Equation 2.12 may now be written alternatively by substitution of this result:

$$(1 - C_{D_L})d \log C_L - C_{D_M} d \log M = 0 \quad (2.17)$$

The partial optima for C_L or M are obtained by setting $dC_L=0$ or $dM=0$ —alternatively $d \log C_L=0$ or $d \log M = 0$ —resulting in

$$\text{constant } M : C_{D_L} = 1 \rightarrow \frac{\partial C_D}{\partial C_L} = \frac{C_D}{C_L} \rightarrow C_L = C_{L,md} \quad (2.18)$$

$$\text{constant } C_L : C_{D_M} = 0 \rightarrow \frac{\partial C_D}{\partial M} = 0 \quad (2.19)$$

The first of these partial optima can be allocated in the drag polar(s)—see Figure 2.3a—by means of a tangent from the origin, the second is relevant only for high speed aircraft where $C_{D_M} = 0$ defines a relationship between C_L and M as illustrated by Figure 2.2b. However, in most cases the drag at subcritical speeds is defined as a unique polar—hence $C_{D_M} = 0$ —up to a certain Mach number. Above this speed $C_{D_M} > 0$ and the lift/drag ratio is generally degraded.

The condition for an *unconstrained* maximum value of L/D is that both partial optima occur at the same time. Hence the combination of $C_{D_L} = 1$ and $C_{D_M} = 0$ defines a unique condition for $(L/D)_{max}$ only in the case that a maximum or a minimum exists for a given lift coefficient. In Figure 2.2b this condition is identified as Point A, with $L/D = 18.40$. If, on the other hand, for low subsonic speeds there is only one drag polar, the aircraft has a constant maximum lift/drag ratio defined by $C_L = C_{L,md}$.

For the case of parabolic drag polars, generally with coefficients dependent on the Mach number,

$$C_D = C_{D,0}(M) + K(M)C_L^2 \quad \text{with} \quad K(M) \stackrel{\text{def}}{=} dC_D/d(C_L^2) \quad (2.20)$$

the conditions for minimum drag for given Mach number are

$$C_{L,md} = \sqrt{C_{D,0}(M)/K(M)} \quad (2.21)$$

$$C_{D,md} = 2C_{D,0}(M) \quad (2.22)$$

$$(L/D)_{md} = \frac{1}{2\sqrt{K(M)C_{D,0}(M)}} \quad (2.23)$$

For this case the logarithmic derivative C_{D_L} is

$$C_{D_L} = \frac{2K(M)C_L^2}{C_{D,0}(M) + K(M)C_L^2} = 2 \frac{\text{Induced Drag}}{\text{Total Drag}} \quad (2.24)$$

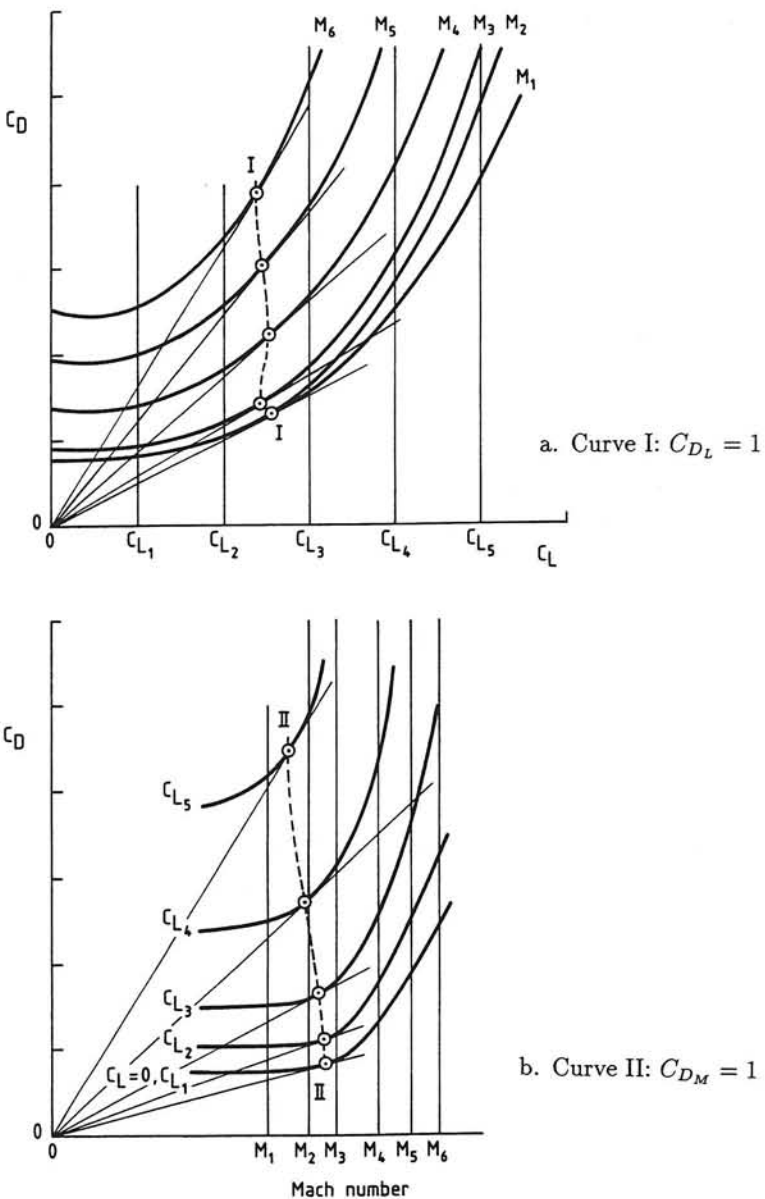


Figure 2.3: Graphical construction of conditions $C_{D_L} = 1$ and $C_{D_M} = 1$

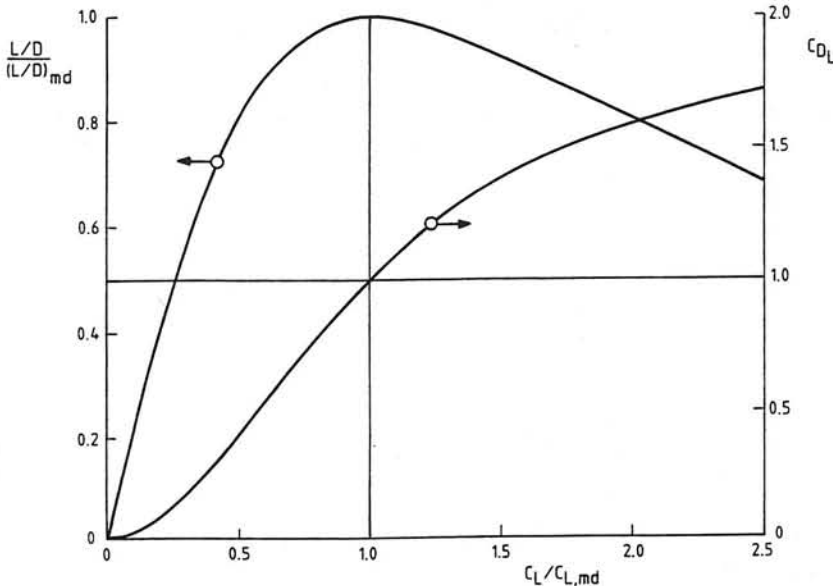


Figure 2.4: Generalized drag properties for parabolic polars

and for $C_{D_L} = 1$ the well known result is obtained that the induced drag and the zero-lift drag are equal. The relationship between C_{D_L} and the lift coefficient is:

$$C_{D_L} = 2 \frac{(C_L/C_{L,md})^2}{1 + (C_L/C_{L,md})^2} \rightarrow \frac{C_L}{C_{L,md}} = \sqrt{\frac{C_{D_L}}{2 - C_{D_L}}} \quad (2.25)$$

and the lift to drag ratio—in relation to its maximum value—amounts to

$$\frac{L/D}{(L/D)_{md}} = \frac{2(C_L/C_{L,md})}{1 + (C_L/C_{L,md})^2} = \sqrt{C_{D_L}(2 - C_{D_L})} \quad (2.26)$$

These interrelationships are depicted in a generalized form in Figure 2.4, which applies to low subsonic as well as high subsonic speeds, provided that drag polars can be approximated by Equation 2.20 at any Mach number (including the drag rise). However, for a cambered wing the term drag coefficient at zero lift is not very meaningful. For the purpose of performance computation at subcritical speeds Equation 2.20—representing a symmetric drag polar—is usually adequate. For high speeds a better approximation is for example

$$C_D = C_D^*(M) + K^*(M)(C_L - C_L^*)^2 \quad (2.27)$$

with C_L^* denoting the lift coefficient for minimum drag coefficient C_D^* , and K^* denotes a modified (higher) induced drag factor than K used in Equation 2.20.

2.2 Constraints on Altitude or Thrust

Altitude constraint: in a practical situation where for an aircraft (given AUW) flying at a specified altitude the condition of minimum drag is sought, the results of the previous section are not valid if the resulting Mach number is in the drag rise. Since for this condition $L = W$ dictates that

$$C_L M^2 = \frac{W/S}{\frac{1}{2} \gamma p} = \text{constant} \quad (2.28)$$

the following constraint on C_L and M applies

$$d \log C_L + 2d \log M = 0 \quad (2.29)$$

Substitution into Equation 2.17 yields

$$C_{D_L} = 1 + 1/2 C_{D_M} \quad (2.30)$$

For low-subsonic speeds C_{D_M} is usually negligible—except for high lift coefficients—and this result is identical to Equation 2.18. As soon as the drag rise is entered, C_{D_M} increases and hence $C_{D_L} > 1$ and $C_L > C_{L,md}$. This is illustrated in Figure 2.2b where curves of constant $C_L M^2$ have been drawn and their points of tangency to the L/D contours have been constructed, defining the maximum according to Equation 2.30. The example shows that for $M > 0.65$ Equation 2.30 begins to diverge from Equation 2.18; this divergence starts at point A, corresponding to $C_L M^2 = 0.215$. In the present example the altitude for which Equation 2.30 has to be applied is defined by $p < 2W/(0.215\gamma S)$, or $p < 6.64W/S$.

For higher cruise altitudes—hence lower ambient pressures—than point A the condition for maximum L/D at given altitude is found by intersecting the appropriate curve $C_L M^2 = \text{constant}$ with Equation 2.30, as depicted in Figure 2.2b. The flight Mach number for maximum L/D corresponding to this altitude is lower than the Mach number for $C_{L,md}$ defined by Equation 2.11. For example, in the same figure a selected condition $C_L M^2 = 0.35$ intersects Equation 2.30 in Point B—the combination $C_L = 0.57$, $M = 0.78$ —where $L/D \approx 17.0$. This lift coefficient is considerably higher than $C_{L,md}$ for the same Mach number and hence the conditions for minimum drag are not correctly calculated when Equations 2.10 and 2.11 are used.

Thrust constraint: this case is important when a flight condition is to be determined which results in minimum drag for given engine rating, since it will result in minimum thrust and hourly fuel consumption. An engine thrust rating limit is approximately equivalent to a constraint on the corrected thrust²,

$$\frac{T}{\delta} = \frac{D}{\delta} = 1/2\gamma p_{sl} M^2 C_D S = \text{constant} \quad (2.31)$$

²For details see Section 4.1.

This constraint can be interpreted as

$$C_D M^2 = \text{constant} \rightarrow d \log C_D + 2d \log M = 0 \quad (2.32)$$

Expanding $d \log C_D$ in terms of the C_L - and M -derivatives in accordance with Equation 2.16 yields the following condition for minimum drag:

$$C_{D_L} d \log C_L + (2 + C_{D_M}) d \log M = 0 \quad (2.33)$$

After substitution into Equation 2.17 the result appears—perhaps not surprisingly—to be identical to Equation 2.30:

$$C_{D_L} = 1 + 1/2 C_{D_M}$$

. For a selected value of $C_D M^2 = 0.02$ point C in Figure 2.2b corresponds to this condition. If the aircraft flies in the drag rise this condition again does not result in the Minimum Drag condition defined by Equations 2.10 and 2.11.

In conclusion we find that for a given Mach number the condition for maximum L/D is $C_{D_L} = 1$, whereas for an altitude or thrust constraint one finds $C_{D_L} = 1 + 1/2 C_{D_M}$. At subcritical speeds these two conditions are compatible only for $\partial C_D / \partial M = 0$. At high subsonic speeds they result in different combinations of lift coefficient and Mach number, but always with a lower L/D than at subcritical Mach numbers. However, the conclusion that optimum flight should take place at Point A in Figure 2.2b is not justified, because for jet and turbofan powered aircraft the engine efficiency is also variable with Mach number. For long range flights the condition for minimum drag is not the most interesting case, as will be shown in the following chapter.

Chapter 3

The Parameter ML/D

The Specific Range¹ \mathcal{SR} is the instantaneous value of distance covered per unit quantity of fuel consumed for a given aircraft weight, speed and altitude,

$$\mathcal{SR} \stackrel{\text{def}}{=} \frac{\Delta R}{\Delta W_F} = \frac{\Delta R / \Delta t}{\Delta W_F / \Delta t} = \frac{V}{F} \quad (3.1)$$

where F denotes the fuel weight consumed per unit time. Integration of the \mathcal{SR} over a given flight trajectory—for a change of aircraft weight equal to the fuel consumed—gives the range. Introducing the Thrust Specific Fuel Consumption TSFC for jet or turbofan engines:

$$C_T \stackrel{\text{def}}{=} \frac{F}{T} \quad (3.2)$$

and noting that in steady cruising flight it can be assumed that Lift is equal to Weight and Thrust is equal to Drag, the \mathcal{SR} can be rewritten as follows:

$$\mathcal{SR} = \frac{a_{sl}}{W} \frac{ML/D}{C_T/\sqrt{\theta}} \quad (3.3)$$

where a_{sl} and θ denote the speed of sound at Sea Level ISA and the relative ambient temperature, respectively. The term $C_T/\sqrt{\theta}$ is usually referred to as the "Corrected Specific Fuel Consumption". For a given engine rating and Mach number this parameter is constant in the stratosphere, and its variation below the tropopause is generally small for altitudes above 9 150 m (30 000 ft). Although the variation of TSFC with Mach number is by no means negligible—especially for high bypass ratio turbofans—the parameter ML/D is often used for defining the Mach number for maximum \mathcal{SR} . The resulting flight condition appears to be fairly accurate for idealized jet engine propulsion, provided the Mach number range under consideration is not too large². In this section the condition for maximum ML/D will be analyzed in terms of logarithmic derivatives:

$$d \log M + d \log C_L - d \log C_D = 0 \quad (3.4)$$

¹Since the effects of wind are not considered in this report the Specific Range is identical to the Specific Air Range.

²The Specific Range treated in Chapter 4 is a more general criterion for optimum range performance.

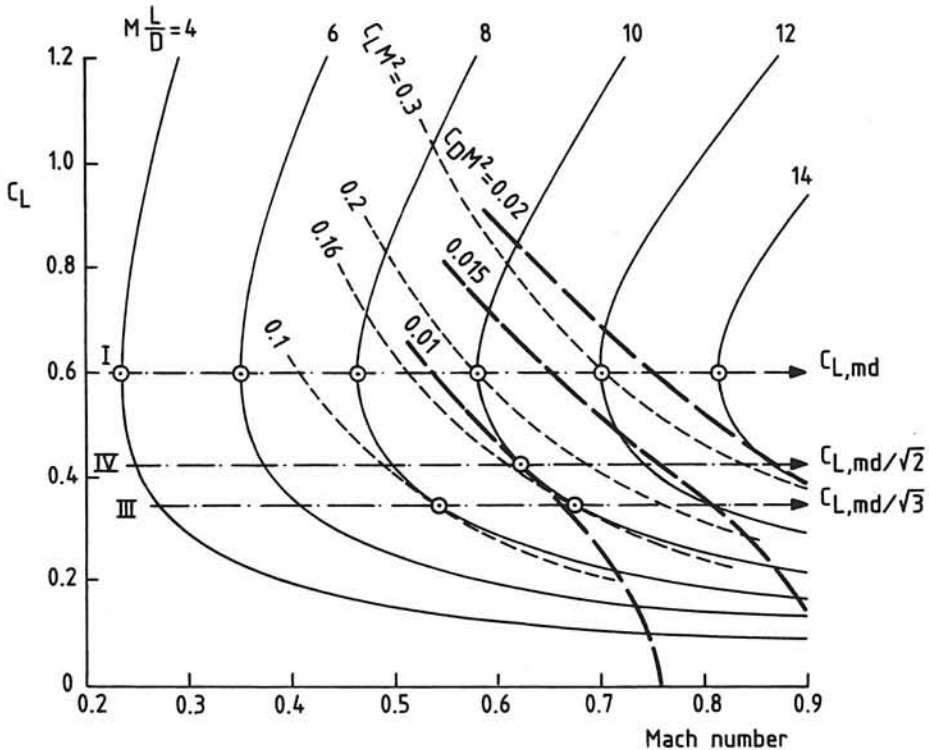


Figure 3.1: The factor ML/D at subcritical speeds

Expanding $d \log C_D$ in terms of the lift coefficient and Mach number using Equation 2.16 one finds

$$(1 - C_{D_L})d \log C_L + (1 - C_{D_M})d \log M = 0 \quad (3.5)$$

where the logarithmic derivatives C_{D_L} and C_{D_M} are defined by Equations 2.14 and 2.15.

3.1 Maximum ML/D at Subcritical Speeds

Although compressibility drag will be present at high subsonic Mach numbers, the case $C_{D_M} = 0$ will be treated as an instructive example. Figure 3.1 shows contours of constant ML/D in the lift coefficient versus Mach number plane for the case of a single parabolic drag polar. For given lift coefficient the lift/drag ratio is independent of the Mach number, and ML/D increases monotonically with the Mach number, leading to the following observations:

- For each Mach number the minimum drag has the same value—defined by $C_{D_L} = 1$, or $C_L = C_{L,md}$ —and $M(L/D)_{md}$ increases proportional to M .

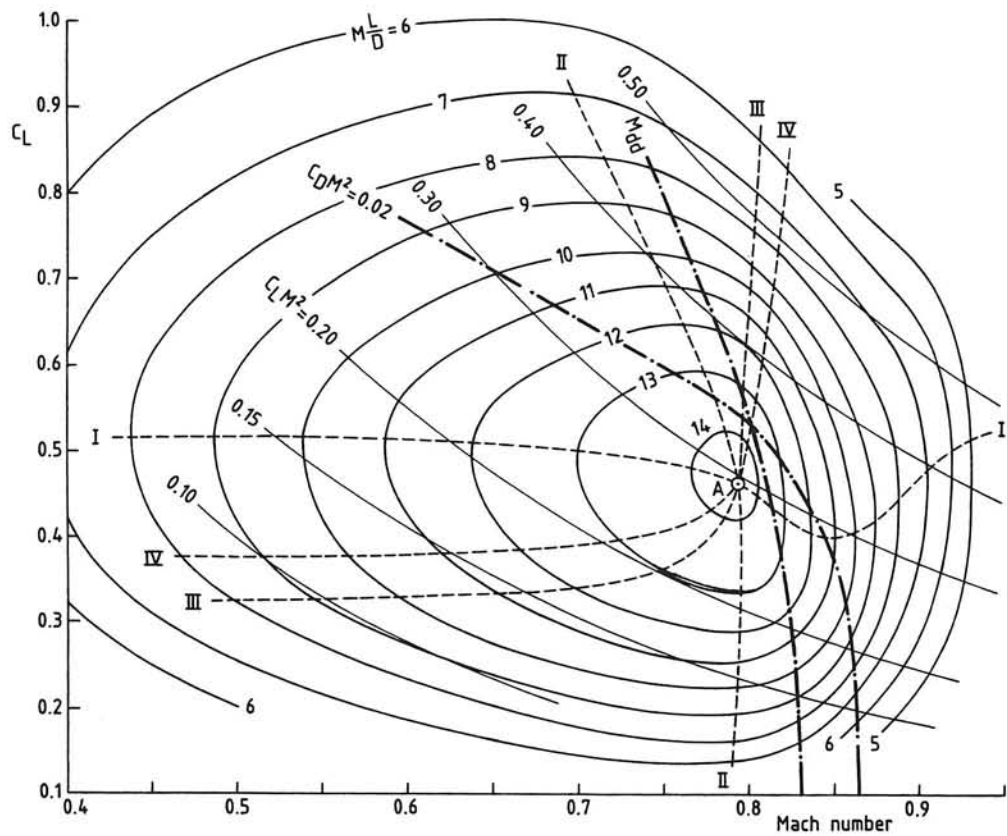


Figure 3.2: The factor ML/D with compressibility effects

- For a given lift coefficient there is no partial optimum for the Mach number and the parameter ML/D does not have an unconstrained maximum.

This means that—if the engines deliver unlimited thrust and TSFC is not affected by the Mach number—the aircraft will continue to improve its \mathcal{SR} with increasing Mach number, and for constant lift coefficient the altitude will also increase. However, in practice there will always be at least one of the following constraints.

Altitude constraint: $C_L M^2$ is constant and Equation 2.29 will apply. Substitution into Equation 3.5 yields

$$C_{D_L} = 1/2 \quad (\text{for } C_{D_M} = 0) \quad (3.6)$$

This result is identical to the well known maximum of C_L/C_D^2 . For a parabolic drag polar Equation 2.25 yields accordingly: $C_L = C_{L,md}/\sqrt{3}$, as indicated by Line III in Figure 3.1.

Thrust constraint: the condition $C_D M^2 = \text{constant}$ applies and Equation 2.32 will apply. Substitution into Equation 3.5 yields

$$C_{D_L} = 2/3 \quad (\text{for } C_{D_M} = 0) \quad (3.7)$$

which is identical to the well known maximum of C_L^2/C_D^3 . For a parabolic drag polar the result is: $C_L = C_{L,md}/\sqrt{2}$, indicated by Line IV in Figure 3.1.

In conclusion we find that the case $C_{D_M} = 0$ provides useful results only for constrained optimization. For *parabolic drag polars* the result is summarized in the following table.

case	C_{D_L}	C_L	Curve in Fig. 3.1
$M=\text{constant}$	1	$C_{L,md}$	I
$W/\delta=\text{constant}$	$1/2$	$C_{L,md}/\sqrt{3}$	III
$T/\delta=\text{constant}$	$2/3$	$C_{L,md}/\sqrt{2}$	IV

These conditions are clearly incompatible, confirming the absence of an unconstrained optimum for this hypothetical case, which is treated frequently in textbooks on flight performance.

3.2 ML/D with Compressibility Effects

Partial and unconstrained optima: the situation depicted in Figure 3.1 remains valid up to the Mach number where compressibility effects on the drag are becoming

manifest, i.e. in the case illustrated by Figure 2.1 up to $M \approx 0.65$. Figure 3.2 illustrates that contours of constant ML/D are drastically different in the drag rise: they become closed curves and there appears an unconstrained optimum for the lift coefficient ($C_L = 0.465$) and the Mach number ($M = 0.795$)—approximately 0.015 below the drag divergence Mach number—where ML/D reaches a value of about 14.0: Point A. For this flight condition $L/D = 17.61$, or 95.7% of $(L/D)_{\max} = 18.40$.

The partial optimum for given Mach number (Curve I) is obviously the same as that for maximum L/D at given Mach number, but due to compressibility effects there is now also a partial optimum for given lift coefficient: $C_{D_M} = 1$ (Curve II). Its governing equation can be derived from Equation 3.5. Curves I and II intersect at Point A, the unconstrained maximum of ML/D .

Altitude constraint: for constant $C_L M^2$ the optimum is found by substitution of Equation 2.29 into Equation 3.5, resulting in

$$C_{D_L} = 1/2 (1 + C_{D_M}) \quad (3.8)$$

identified in Figure 3.2 as Curve III. For low Mach numbers ($C_{D_M} = 0$) this equation is identical to the result found in Subsection 3.1 but for $M > 0.65$ —in the present example—there is a rapid increase in C_{D_L} and in C_L , resulting in a bent-up branch of Curve III, intersecting Curves I and II in point A. It should also be noted that for Mach numbers in excess of Point A the optimum for specified altitude occurs at $C_L > C_{L,md}$, as opposed to the case of subcritical speeds.

Thrust constraint: the optimum can be found by substitution of Equations 2.32 and 2.16 into Equation 3.5,

$$C_{D_L} = 1/3 (2 + C_{D_M}) \quad (3.9)$$

This Curve IV—see Figure 3.2—again intersects the other partial optima in point A. This can be verified by combining Equations 3.8 and 3.9 resulting in $C_{D_L} = C_{D_M} = 1$.

Graphical solution: although the location of the unconstrained optimum (point A) in the lift coefficient versus Mach number plane has been illustrated by means of iso- ML/D contours, its determination does not require these contours. A graphical solution using the drag polar—see Figure 2.3—provides a direct solution as follows.

- The condition $C_{D_L} = 1$ is identical to $\partial C_D / \partial C_L = C_D / C_L$ for constant Mach number. The solution is found graphically by means of a tangent construction, see Figure 2.3a.
- Similarly a tangent construction is applied to $\partial C_D / \partial M = C_D / M$ for constant C_L , see Figure 2.3b.
- Both conditions are transferred to the C_L versus M plane (see Figure 3.2): Curves I and II, intersecting in Point A.

In conclusion an unconstrained flight condition for maximum ML/D exists only when compressibility effects are present, and as a consequence it is located in the drag rise. For the example aircraft the criterion $\partial C_D / \partial M = C_D/M$ defines a slope of approximately 0.033, as opposed to the usual definition for the drag divergence Mach number: $\partial C_D / \partial M = 0.10$. In the next section it will be shown that a similar criterion applies to the maximum \mathcal{SR} of high speed jet aircraft.

Chapter 4

The Specific Range

The parameter ML/D treated in the previous section is useful in the case that variations in the TSFC are negligible, but this is usually not the case when accurate results are required or Mach number variations are large. In that case it is appropriate to introduce the variation of the overall powerplant efficiency,

$$\eta \stackrel{\text{def}}{=} \frac{\text{Net Propulsive Power}}{\text{Heat Content of Fuel Flow}} = \frac{TV}{\dot{m}_F H} = \frac{TV}{FH/g} \quad (4.1)$$

where \dot{m}_F denotes the mass flow rate of the fuel with calorific value H . The relation between the overall powerplant efficiency and the TSFC for jet and turbofan engines is as follows,

$$\eta = \frac{a_{sl}}{H/g} \frac{M}{C_T/\sqrt{\theta}} \quad (4.2)$$

Substitution into Equations 3.1 and 3.3 yields

$$\mathcal{SR} = \frac{V}{F} = \frac{R_H}{W} \eta L/D \quad (4.3)$$

where $R_H \stackrel{\text{def}}{=} H/g$ amounts to approximately 4 400 km (2 376 nm) for typical gas turbine engine fuel¹. The last equation shows that for given aircraft AUW the maximum value of the **Range Parameter**,

$$\mathcal{P} \stackrel{\text{def}}{=} \eta L/D = \frac{WV}{R_H F} \quad (4.4)$$

results in the maximum Specific Range. Since the overall powerplant efficiency has basically the same definition for propeller aircraft and for turbojet or turbofan aircraft, the Range Parameter is a more significant parameter than ML/D since it covers the complete range of transport aircraft powerplants. In particular for making a comparison between

¹In that case Equation 4.1 yields $\eta = 0.2788M/(C_T/\sqrt{\theta})$.

subsonic and supersonic cruising aircraft it is not acceptable to use ML/D instead of the Range Parameter.

The objective of the cruise point optimization is to find a maximum of the product of the powerplant efficiency η and the aerodynamic fineness L/D . Since both quantities are mutually unrelated functions of the airspeed and altitude, the combined optimum does not generally coincide with any of the maxima for η or L/D , provided these exist.

4.1 Generalized Engine Performance

The engine thrust and fuel consumption—and hence the overall powerplant efficiency—are basically functions of the altitude², the airspeed and the engine rating. Textbooks on gasturbine engine performance show that the generalized performances of turbojet and turbofan engines can be described in generalized equations as follows,

$$\text{Corrected Thrust : } \frac{T}{\delta} = f_1(M, N/\sqrt{\theta}) \quad (4.5)$$

$$\text{Corrected Fuel Flow : } \frac{F}{\delta\sqrt{\theta}} = f_2(M, N/\sqrt{\theta}) \quad (4.6)$$

where δ denotes the relative ambient pressure and $N/\sqrt{\theta}$ is the corrected High Pressure Rotor RPM. The latter can be eliminated to yield

$$\frac{F}{\delta\sqrt{\theta}} = f_3(M, T/\delta) \quad (4.7)$$

and by substitution into Equation 4.1 we obtain

$$\eta = M \frac{a_{sl}}{R_H} \frac{T/\delta}{F/(\delta\sqrt{\theta})} = f_4(M, T/\delta) \quad (4.8)$$

Hence, for variable engine rating it is found that the overall powerplant efficiency is determined by the flight Mach number and the Corrected Thrust. It can also be shown [25] that Equation 4.8 holds for any gasturbine-based propulsion system with propeller power and/or jet thrust output, provided effects due to Reynolds number variation and installation effects are ignored. Figure 4.1 is a representative example of the overall powerplant efficiency of a present day turbofan engine, showing the effects of Mach number variation and the engine rating parameter $T/(\delta T_{to})$. The latter compares the Corrected Thrust to the maximum take off Thrust for the Sea Level ISA static condition, T_{to} . For typical turbofan engine cruise conditions this rating parameter varies between approximately 0.8 and 1.1. The maximum cruise rating has also been indicated in the diagram for altitudes near 35 000 ft (10 668 m)³. Figure 4.1 shows that the Mach number has a much larger effect on the powerplant efficiency variation than the engine rating. Hence the case that the powerplant efficiency is a function of the Mach number only will be considered first.

²For standard atmospheric conditions the altitude defines a combination of ambient pressure and temperature.

³In fact this curve is a limitation by the engine RPM.

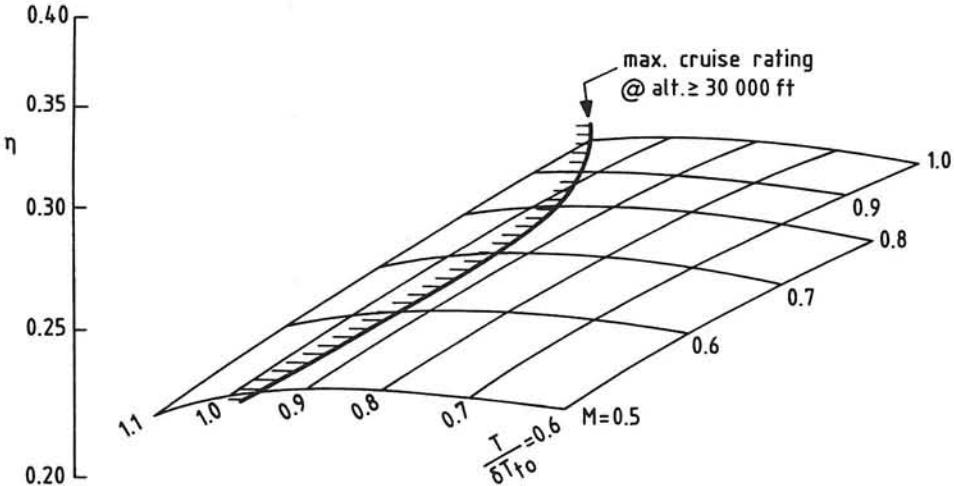


Figure 4.1: Engine performance of a high bypass turbofan engine

4.2 Maximum range parameter

In order to find conditions of maximum \mathcal{SR} it appears appropriate to introduce the following log-derivative, for the case that the efficiency is a function of the Mach number only:

$$\eta_M \stackrel{\text{def}}{=} \frac{d \log \eta}{d \log M} = \frac{M}{\eta} \frac{d \eta}{d M} \quad (4.9)$$

This parameter generally varies between zero for propulsion with efficiency independent of the flight speed, and one for the (theoretical) case of constant TSFC⁴. The condition for maximum \mathcal{SR} may now be derived from logarithmic differentiation of Equation 4.4:

$$d \log \mathcal{P} = d \log \eta + d \log C_L - d \log C_D = 0 \quad (4.10)$$

which can be expanded in terms of partial derivatives:

$$(1 - C_{D_L}) d \log C_L + (\eta_M - C_{D_M}) d \log M = 0 \quad (4.11)$$

It is noted that for $\eta_M = 1$ —and hence constant TSFC—this equation is the equivalence of Equation 3.5, the condition for maximum ML/D .

⁴See Section 4.3 for further explanation.

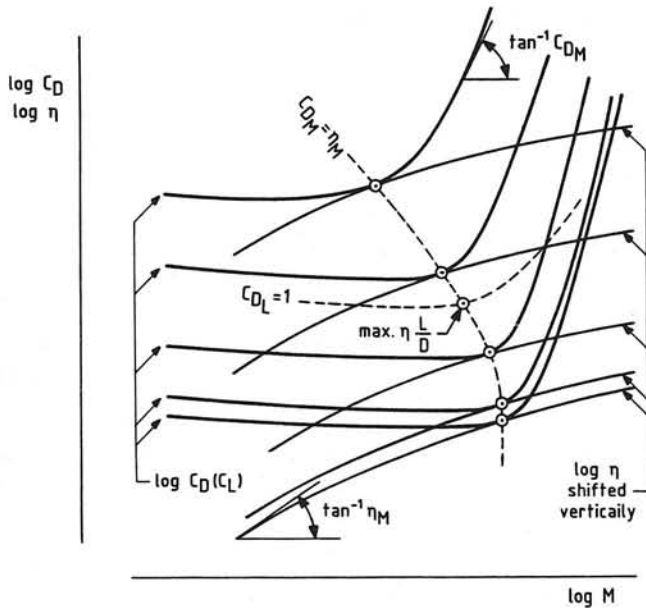


Figure 4.2: Graphical construction of the condition $C_{D_M} = \eta_M$

Partial and unconstrained optima: for C_L and M the partial optima are obtained from Equation 4.11,

constant Mach number:	$C_{D_L} = 1$
constant lift coefficient:	$C_{D_M} = \eta_M$

The first of these partial optima is identical to the case of maximum ML/D , the second can be rewritten alternatively,

$$\frac{\partial C_D}{\partial M} = \eta_M \frac{C_D}{M} \quad (4.12)$$

Since both the Mach number and the drag coefficient are positive and generally C_{D_M} is either zero or positive, there can be two solutions:

1. $\eta_M > 0 \rightarrow \partial C_D / \partial M > 0$, defining an optimum condition in the drag rise;
2. $\eta_M = 0 \rightarrow \partial C_D / \partial M = 0$, with an optimum defined by the condition $C_{D_M} = 0$ (see Figure 2.2b), or with an underdetermined optimum Mach number in case there is one (low speed) drag polar.

The interpretation of this result is as follows:

- If the overall efficiency is *independent of the Mach number*, the range parameter has its maximum value—for any subcritical Mach number—when $C_L = C_{L,md}$. The maximum specific range has the same value for different altitudes, provided the airplane flies at the Minimum Drag Speed and the efficiency is also independent of the altitude.
- If the overall efficiency *reaches a maximum value* for a subcritical Mach number, say $M_{\eta-opt}$, the maximum specific range occurs at this flight speed, and the pressure altitude is defined by

$$p = \frac{2W/S}{\gamma M_{\eta-opt}^2 C_{L,md}} \quad (4.13)$$

- If the overall efficiency increases continuously with Mach number, the condition $C_{D_M} = \eta_M$ must be combined with the condition $C_{D_L} = 1$, in order to find the unconstrained optimum.

The flight condition defined by $C_{D_M} = \eta_M$ can be found numerically or graphically. An example of a graphical approach is shown on Figure 4.2 where a log-log scale has been used in accordance with the use of logarithmic derivatives. The points where the slopes of $\log C_D$ are equal to the slopes of $\log \eta$ define the solution of Equation 4.12.

An example of iso- \mathcal{P} curves in the C_L versus M plane is shown on Figure 4.3 with partial optima for C_L and M , indicated as Curves I and II, respectively. Although the general shape of this diagram is similar to Figure 3.2 for ML/D there are some noticeable differences.

- Since $\eta_M < 1$, the unconstrained optimum (point A) is at a lower Mach number than point A for maximum ML/D —approximately 0.045 below the drag divergence Mach number—while the optimum itself is not so sharp.
- For subcritical Mach numbers the constrained optima for constant W/δ and T/δ —Curves III and IV respectively—occur at higher values of the lift coefficient compared to Figure 3.2. This will be explained in the following paragraphs.

Altitude constraint: the maximum value of \mathcal{P} is obtained by substituting $C_L M^2 = \text{constant}$ (or $d\log C_L + 2d\log M = 0$) into Equation 4.11, which yields

$$C_{D_L} = 1 + 1/2 (C_{D_M} - \eta_M) \quad (4.14)$$

In Figure 4.3 this equation is represented by Curve III. Its intersection with the appropriate value of $C_L M^2$ defines the constrained optimum, Point B. In the case of a *drag polar without compressibility effects* ($C_{D_M} = 0$) Equation 4.14 has the following solution,

$$C_{D_L} = 1 - \eta_M/2 \quad (4.15)$$

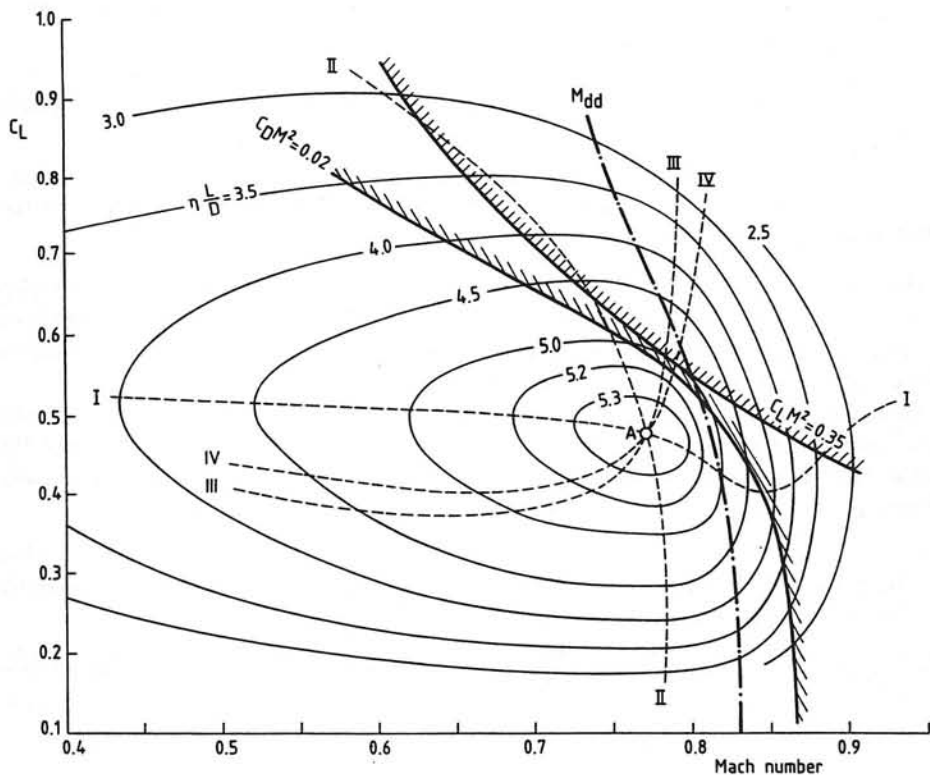


Figure 4.3: Variation of the Range Parameter

Usually the drag polar is a parabola at low speeds, hence from Equation 2.25

$$C_L = C_{L,md} \left(\frac{2 - \eta_M}{2 + \eta_M} \right)^{1/2} \rightarrow M = M_{md} \left(\frac{2 + \eta_M}{2 - \eta_M} \right)^{1/4} \quad (4.16)$$

with M_{md} defined by Equation 2.11. The corresponding lift/drag ratio according to Equation 2.26 is

$$L/D = 1/2 \sqrt{4 - \eta_M^2} (L/D)_{md} \quad (4.17)$$

This result covers various classical optima: $C_L = C_{L,md}/\sqrt{3}$ for constant corrected TSFC ($\eta_M = 1$), and $C_L = C_{L,md}$ for constant overall propulsive efficiency ($\eta_M = 0$). For modern turbofan engines η_M is typically between 0.4 and 0.6⁵. Equations 4.14 and 4.16 are therefore useful generalisations of the classical flight-mechanical criteria, applicable to arbitrary propulsion systems, though applicable to low speeds only.

Thrust constraint: the maximum of \mathcal{P} is obtained by combining Equation 4.11 and Equation 2.32, yielding the following result:

$$C_{D_L} = \frac{2 + C_{D_M}}{2 + \eta_M} \quad (4.18)$$

An example of a constrained optimum is Point *C* in Figure 4.3. In the case of *zero compressibility* Equation 4.18 has the following solution:

$$C_{D_L} = (1 + \eta_M/2)^{-1} \quad (4.19)$$

At *subcritical speeds* the drag polar is usually parabolic. In that case Equation 2.25 applies and the result is the following condition for the optimum lift coefficient,

$$C_L = C_{L,md}/\sqrt{1 + \eta_M} \rightarrow M = M_{md} \sqrt{\frac{1 + \eta_M}{1 + \eta_M/2}} \quad (4.20)$$

where in this case the Minimum Drag Mach number is determined by the drag coefficient for the minimum drag condition instead of the lift coefficient⁶:

$$M_{md} = \sqrt{\frac{2T/S}{\gamma p C_{D,md}}} \quad (4.21)$$

The lift/drag ratio according to Equation 2.26 is

$$L/D = \frac{\sqrt{1 + \eta_M}}{1 + \eta_M/2} (L/D)_{md} \quad (4.22)$$

This result is again in accordance with classical criteria: $C_L = C_{L,md}/\sqrt{2}$ for constant TSFC, and $C_L = C_{L,md}$ for constant powerplant efficiency.

⁵The actual value is not entirely independant of the Mach number; see Section 4.3.

⁶For further explanation reference is made to [27].

For turboprop engines the engine rating is based on the engine output shaft power P_{br} instead of the thrust. In that case a more logical combination of independent variables is the Mach number and the corrected power,

$$\eta = \eta \left(M, \frac{P_{br}}{\delta\sqrt{\theta}} \right) \quad (4.23)$$

The results for the various partial optima may now be derived analogous to the previous case. Only one result will be mentioned here: the optimum for constant Corrected Power $P_{br}/(\delta\sqrt{\theta}) = C_D \frac{1}{2} \gamma p_{sl} a_{sl} M^3 S$, hence $d\log C_D + 3d\log M = 0$. For this case Equation 4.11 yields

$$C_{D_L} = \frac{3 + C_{D_M}}{3 + \eta_M} \quad (4.24)$$

For a *parabolic drag polar* and zero compressibility this is equivalent to:

$$C_L = C_{L,md} / \sqrt{1 + 2\eta_M/3} \quad (4.25)$$

a result that is directly comparable to Equation 4.20. This case may be assumed to apply to turboprop or prop-fan powered aircraft where η_M has a small positive or negative value near the subcritical cruise Mach number.

Multivalued optimum solutions. It is possible that the conditions for partial optima do not result in a unique solution. For example, supersonic cruising aircraft—not treated in the present report—may have maxima for L/D and V/F both at subsonic and supersonic speeds. Subsonic aircraft may also have anomalies in the drag polars, for example when a shock-free condition with low drag occurs in a small region of Mach numbers. This behaviour will be clearly manifest in the drag polars, making the analyst aware of the situation. In such a case both local maxima for $\eta L/D$ must be studied in detail and compared to find the highest value [17]. For supersonic cruising aircraft good subsonic range performance is also of paramount importance, and both the subsonic and supersonic optima are of practical significance.

4.3 Interpretation of the Derivative η_M

The logarithmic derivative η_M introduced in the previous section effectively denotes the corresponding percentage change in efficiency divided by the corresponding percentage change in Mach number. It can be related to the corrected TSFC as follows,

$$\eta_M = 1 - \frac{M}{C_T/\sqrt{\theta}} \frac{d(C_T/\sqrt{\theta})}{dM} \quad (4.26)$$

This parameter has been used extensively in the analysis to define the optimum flight Mach number and deserves further explanation.

The overall powerplant efficiency may be expressed as the product of a combustion efficiency η_{cb} , a thermal efficiency η_{th} , and a propulsive efficiency η_{pr} ,

$$\eta = \eta_{cb} \eta_{th} \eta_{pr} \quad (4.27)$$

Logarithmic differentiation yields

$$\eta_M = \frac{d \log \eta_{cb}}{d \log M} + \frac{d \log \eta_{th}}{d \log M} + \frac{d \log \eta_{pr}}{d \log M} \quad (4.28)$$

The first of these terms is generally nearly zero, while the second will have a small positive value due to the ram effect at high speeds. The third contribution is the most important one; its value can be associated with the well known expression for the Froude efficiency

$$\eta_{pr} = \frac{2V}{V + v_j} = \frac{2}{1 + v_j/V} \quad (4.29)$$

with v_j denoting the mean exhaust jet velocity. The variation of v_j with the flight Mach number is not readily determined since off-design engine performance analysis is a rather complex problem. However, in general it can be observed that for powerplant installations with a high jet velocity (e.g. idealized jets) this variation is small, while for low exhaust velocities—in the case of very high bypass engines and propeller propulsion—the speed increment $v_j - V$ varies little with airspeed. The following hypothetical cases can therefore be distinguished:

$$\text{constant } v_j : \quad \frac{d \log \eta_{pr}}{d \log M} = \frac{d \log \eta_{pr}}{d \log V} = 1 - \frac{V}{V + v_j} = 1 - \eta_{pr}/2 \quad (4.30)$$

and

$$\text{constant } v_j - V : \quad \frac{d \log \eta_{pr}}{d \log M} = \frac{d \log \eta_{pr}}{d \log V} = 1 - \frac{2V}{V + v_j} = 1 - \eta_{pr} \quad (4.31)$$

Thus it is found that $\eta_M = 1 - \text{factor} \times \eta_{pr}$, where the factor depends primarily on the specific thrust. Since for all cases $\eta_{pr} = 0$ for $M = 0$, η_M approaches 1.0 for $M \downarrow 0$. For subsonic cruise Mach numbers the propulsive efficiency of *turbofan engines* is generally between 0.4 and 0.8 and hence η_M will vary between 0.2 and 0.8. For *propeller powered* aircraft the propulsive efficiency varies only slightly with airspeed and η_M is approximately zero⁷, unless the propellers operate at supersonic tipspeeds. In that case η_M will become negative.

As an example Figure 4.1 shows that for a high-bypass turbofan the constant- T/δ -curves have a nearly constant slope for Mach numbers between 0.6 and 0.9. As the diagram is a double logarithmic plot, this indicates that an exponential relationship for the corrected TSFC can be used as an approximation,

$$C_T/\sqrt{\theta} = \text{constant} \times M^n \quad (4.32)$$

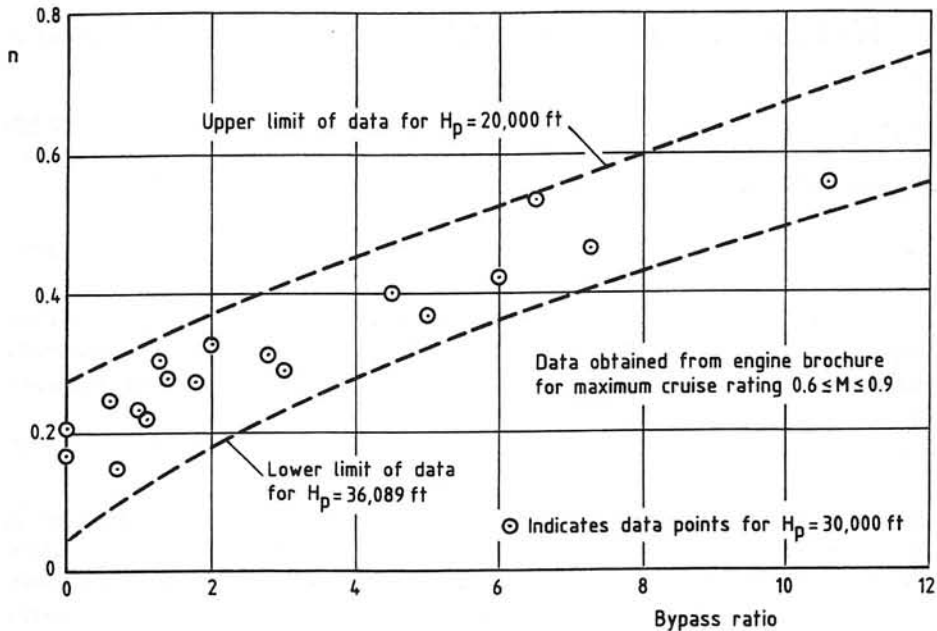


Figure 4.4: The engine efficiency power law exponent

Substitution into Equation 4.26 yields

$$\eta_M = 1 - n \quad (0 \leq n \leq 1) \quad (4.33)$$

Statistical values for the exponent n are given in [2] and have been reproduced in Figure 4.4. In accordance with the derivation given above there appears to be a correlation between n and the bypass ratio—which is related to the specific thrust. An alternative relationship between the corrected TSFC and the Mach number,

$$C_T/\sqrt{\theta} = C_1 + C_2 M \quad (4.34)$$

can be used in Equation 4.26 and it follows that

$$\eta_M = \frac{1}{1 + MC_2/C_1} \quad (4.35)$$

resulting in a value of η_M which is not independent of the Mach number. Although Equation 4.35 provides an accurate approximation over a large range of Mach numbers, Equation 4.33 is usually adequate for cruise performance analysis to derive η_M for a given engine. Figure 4.5 depicts the relation between the overall powerplant efficiency, the corrected TSFC, the log-derivative and the flight Mach number. It illustrates the (in)accuracy of the approximation of a constant η_M for high subsonic speeds.

⁷Note that since $\eta_{prop} < 1$ Equation 4.31 gives a positive value for η_M ; this demonstrates the limited value of the simple analysis.

4.4 Refinements in the Optima

In the previous section only the primary variable for the thrust (the Mach number) has been taken into account. For a more accurate analysis, accounting for the effects of engine rating on efficiency and of Mach number on the maximum cruise thrust, a further extension of the analysis may be required.

Partial and unconstrained optima: the effect of thrust setting is taken into account by means of the following logarithmic derivative:

$$\eta_T \stackrel{\text{def}}{=} \frac{\partial \log \eta}{\partial \log(T/\delta)} = \frac{T/\delta}{\eta} \frac{\partial \eta}{\partial(T/\delta)} \quad (\text{constant Mach number}) \quad (4.36)$$

and since η now depends on two variables we have to modify the definition of η_M accordingly,

$$\eta_M \stackrel{\text{def}}{=} \frac{\partial \log \eta}{\partial \log M} = \frac{M}{\eta} \frac{\partial \eta}{\partial M} \quad (\text{constant } T/\delta) \quad (4.37)$$

The condition for maximum \mathcal{SR} according to Equation 4.11 must now be modified into⁸:

$$\begin{aligned} d \log \mathcal{P} &= (1 - C_{D_L} + \eta_T C_{D_L}) d \log C_L \\ &\quad + (\eta_M - C_{D_M} + 2\eta_T + \eta_T C_{D_M}) d \log M = 0 \end{aligned} \quad (4.38)$$

The *partial optima* with respect to C_L and M are obtained by setting the bracketed terms equal to zero:

$$\text{constant } M \rightarrow C_{D_L} = \frac{1}{1 - \eta_T} \quad (4.39)$$

$$\text{constant } C_L \rightarrow C_{D_M} = \frac{\eta_M + 2\eta_T}{1 - \eta_T} \quad (4.40)$$

The *unconstrained optimum* can be found when these partial optima are combined. This will generally require a numerical iterative solution.

Altitude constraint: the condition $C_L M^2$ constant, or $d \log C_L + 2d \log M = 0$, is substituted into Equation 4.38 yielding

$$C_{D_L} = 1 + 1/2 \left(C_{D_M} - \frac{\eta_M}{1 - \eta_T} \right) \quad (4.41)$$

The solution for the optimum flight condition may now be obtained iteratively by first assuming $\eta_T = 0$, resulting in a first order approximation for the lift coefficient and the Mach number, and hence T/δ . The engine data—see Figure 4.1—will then provide an actual value for η_T and an improved approximation can be obtained.

⁸The derivation can be found in [27].

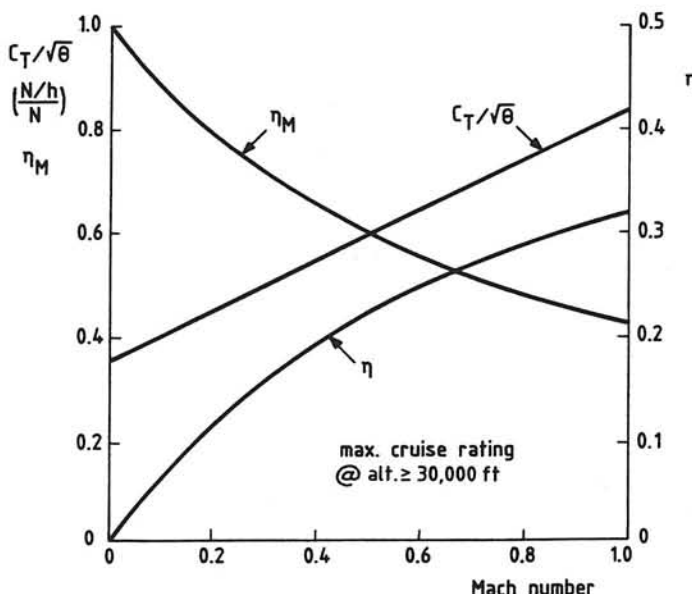


Figure 4.5: Efficiency and TSFC of a high bypass turbofan engine

Constrained optimum for given engine rating: although the case of constant T/δ gives a reasonable approximation for a thrust rating limit, a more accurate analysis may be required for the following reasons:

- An engine rating may refer to an RPM limit, a maximum Turbine Inlet Temperature (TIT), or an Exhaust Gas Temperature (EGT) limit. Not only will the result be a value of $N/\sqrt{\theta}$ which varies with the altitude in the troposphere, but for a given altitude a constant RPM results in a variation of the corrected thrust; see Figure 4.1 as an example.
- For accurate performance analysis it will be necessary to account for installation effects due to inlet total pressure loss, bleed air and power extraction, scrubbing drag and Reynolds number effects. All these effects will not only reduce the overall powerplant efficiency, but they may also introduce an altitude effect on the efficiency for given T/δ .

In this case it will be necessary to first calculate the Mach number versus altitude—hence lift coefficient—limit by means of a numerical or graphical procedure, using the two equilibrium equations: Thrust=Drag, and Lift=Weight. Since this operational limit depends on the aircraft AUW the result is no longer a unique rating limit in the C_L versus M diagram.

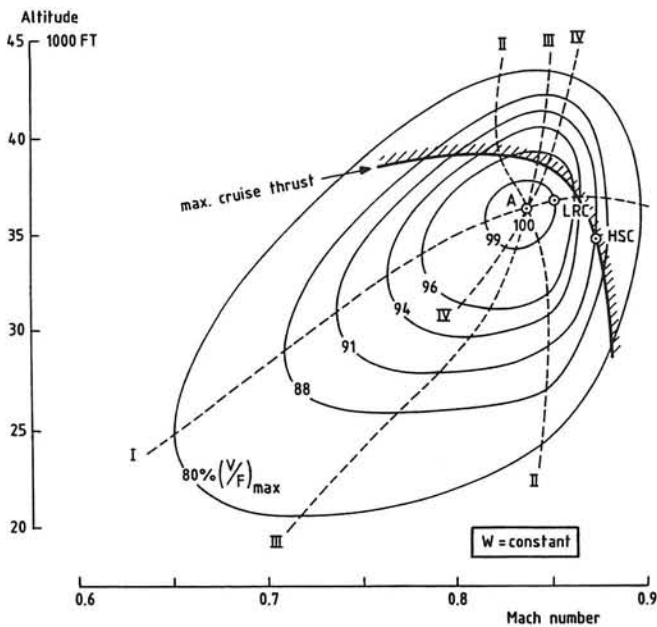


Figure 4.6: The Specific Range affected by operating conditions

Figure 4.6 shows an example of range performance with the \mathcal{SR} plotted versus altitude and Mach number, for a given AUW. For low AUW the maximum \mathcal{SR} appears to be unconstrained (Point A), but for high weights the cruise thrust limit may force the flight condition to a Mach number and altitude below the 100% \mathcal{SR} condition.

Non standard conditions: the engine thrust rating and efficiency are dependent on the Mach number, the pressure and the non standard temperature. Similar to the previous case a numerical analysis is required to identify the best cruise condition for each aircraft weight and the maximum \mathcal{SR} will vary during the cruising flight. Depending on the Thrust/Weight ratio of the aircraft, a temperature above standard may force the aircraft to a considerably reduced altitude or Mach number compared to the 100% maximum \mathcal{SR} condition, resulting in a range performance degradation. This applies in particular to cruising flight after failure of an engine.

Chapter 5

Analysis of Cruising Flight

Different from the problem treated in the previous chapters, dealing with (optimum) instantaneous conditions, the cruise range is an integrated performance. Since there are two control variables at each moment of the flight—we have used the lift coefficient and the Mach number—optimal control laws can be proposed for these variables in order to maximize the range for a given amount of fuel. For the flight crew these control laws have different characteristics and it will be shown that several cruise techniques have serious disadvantages.

Since equilibrium of forces will be assumed during the flight, the result is not necessarily an absolute maximum range. For example, cyclic flight with dolphin type climb and descent profiles may, at least theoretically, increase the range; see [16] and [22]. However, in practice civil transport aircraft fly the cruise sector as a quasi steady flight, with small variations in the control variables. We are therefore interested in approximate solutions for the integrated (optimum) range performance, since they will be adequate for preliminary design purposes. It will be shown that the cruise range can be calculated by means of a simple analytical equation. Conversely, for a specified range the amount of cruise fuel required can be derived in closed form, and from these results the block fuel and the reserve fuel will be obtained readily.

5.1 The Generalized Range Equation

Classical derivations of range are based on either constant propulsive efficiency for propeller aircraft, or constant TSFC for idealized jet propulsion. The pertinent analytical equations can be found in most textbooks on performance. They are usually quite accurate, provided the conditions do not vary considerably during the flight. For example, the following well known expression for the range—attributed to Louis Bréguet (1880-1955)—was derived for *propeller aircraft* cruising at constant altitude and constant angle of attack,

$$R = \frac{\eta_{prop}}{C_P} \frac{C_L}{C_D} \log \frac{W_i}{W_f} \quad (5.1)$$

where "i" and "f" denote the initial and final conditions of the flight. Later, it was found that a very similar equation applies to the range of *jet aircraft* in a cruise/climb with constant speed and constant angle of attack,

$$R = \frac{V}{C_T C_D} \frac{C_L}{W_f} \log \frac{W_i}{W_f} \quad (5.2)$$

In the following text a general expression will be derived for the range of aircraft with various types of gas turbine based powerplants. The range in quasi steady cruising flight is obtained from integration of the specific range,

$$R = \int_{W_f}^{W_i} \frac{V}{F} dW \quad (5.3)$$

For constant \mathcal{SR} during the flight, the range would simply be:

$$R = \frac{V}{F} (W_i - W_f) = \frac{V}{F} W_F \quad (5.4)$$

with W_F denoting the fuel weight. However, due to the decreasing AEW during the flight, the fuel flow is actually decreasing and V/F is increasing. This can be taken into account by using Equation 4.4 for the Specific Range,

$$R = R_H \int_{W_f}^{W_i} \mathcal{P} \frac{dW}{W} \quad (5.5)$$

with \mathcal{P} denoting the Range Parameter. One special solution is found for the case of constant lift coefficient and Mach number—hence constant \mathcal{P} ,

$$R = R_H \mathcal{P} \log(1 - W_F/W_i)^{-1} \quad (5.6)$$

This equation is a generalization of Equations 5.1 and 5.2, since it applies to propeller as well as jet propulsion.

Due to practical operational considerations it is usually impossible to control the flight so that \mathcal{P} is constant. Several alternative techniques have therefore been proposed, resulting in somewhat shorter ranges than Equation 5.6. Although these derivations are covered in many textbooks—see also [2]—for the case of zero compressibility drag, the significant effect of compressibility will be demonstrated as well.

5.2 Range at Subcritical Speeds

This low speed case is obviously most important for propeller aircraft, since jet aircraft have their best performance in the drag rise. But even jet aircraft may be forced to fly at reduced speed and/or altitude, for example when ATC requires this or after engine failure [15]. Especially in the latter case good off-design performance is important in order to reduce the required reserve fuel penalty.

In the following derivations certain combinations of terms are often used and will be designated by the following notations,

$$\zeta \stackrel{\text{def}}{=} W_F/W_i = 1 - W_f/W_i \quad (5.7)$$

$$y \stackrel{\text{def}}{=} C_{L_i}/C_{L,md} \quad (5.8)$$

For subsonic speeds below the drag rise the drag coefficient is usually a unique function of the lift coefficient, hence $C_{L,md}$ is a single number.

Cruise/climb (c/c): flying with constant C_L and M results in a constant C_D —hence constant lift/drag ratio—and constant overall efficiency and corrected TSFC. Thus \mathcal{P} is constant and equal to its initial value, whence

$$R_{c/c} = R_H \mathcal{P}_i \int_{W_f}^{W_i} \frac{dW}{W} = R_H \mathcal{P}_i \log(1 - \zeta)^{-1} \quad (5.9)$$

This flight profile requires the cruise altitude to be steadily increased as fuel is consumed in such a way that W/δ and T/δ remain constant. The relative ambient pressure must therefore decrease proportional to the AUW and in the (isothermal) stratosphere the aircraft flies with constant engine setting. The extra thrust required to increase altitude can be taken into account readily, but for a fair comparison with alternative schedules—at constant altitude—it is preferred to avoid this, assuming that after the cruising flight the aircraft can glide back to the initial altitude, thus regaining the small range loss. As mentioned before the cruise/climb technique will not be acceptable in many situations because of the requirements of ATC.

Horizontal cruise, constant lift coefficient (h,l): this requires the speed of the aircraft to be steadily reduced as fuel is consumed, in such a way that V is proportional to \sqrt{W} . Again L/D is constant and for jet aircraft the Range Parameter varies only due to the decrease in Mach number, and hence the overall efficiency. The engines have to be throttled back so that T varies proportional to W in order to keep T/W constant. If we assume that for that for relatively small speed variations the log-derivative η_M remains constant, the following result is found [28]:

$$R_{h,l} = 2R_H \mathcal{P}_i \{1 - (1 - \zeta)^{\eta_M/2}\} / \eta_M \quad (5.10)$$

This equation covers idealized jet propulsion with $\eta_M = 1$, propeller powered aircraft with $\eta_M = 0$, as well as turbofans with intermediate values of η_M ; see Section 4.3. For jet propulsion Equation 5.10 complies with the classical “square root range equation” which can be written as

$$R = 2R_H \mathcal{P}_i \{1 - \sqrt{1 - \zeta}\} \quad (5.11)$$

For $\eta_M \downarrow 0$ the *numerical values* become equal to Equation 5.9¹.

This flight procedure has several major disadvantages:

¹This can be proven by means of de l'Hôpital's rule.

- For jet propulsion there is a considerable loss in range relative to the cruise/climb procedure due to the deterioration of total efficiency with reducing speed.
- The flight time is increased.
- Steady decrease in speed and continuous variation of the engine setting during the cruise are unlikely to be acceptable to airlines as a normal operational procedure.

Horizontal cruise, constant Mach number (h,M): this is a practical procedure from the operational point of view, because for given altitude a constant Mach number results in constant air speed. During the flight the drag is decreasing due to the weight reduction, and the engines have to be throttled back. This is easily accomplished with modern flight control systems. Integration of the $S\mathcal{R}$ results in the following equation [19] for a *parabolic drag polar*,

$$R_{h,M} = 2R_H \eta_i (L/D)_{md} \{ \arctan y - \arctan y(1 - \zeta) \} \quad (5.12)$$

The difference between the two angles in this equation can be evolved by means of goniometric equations into a single angle. After introduction of the Range Parameter for the initial cruise condition one finds:

$$R = R_H \mathcal{P}_i (y^{-1} + y) \arctan \left\{ \frac{\zeta}{y^{-1} + y(1 - \zeta)} \right\} \quad (5.13)$$

Since for optimum cruising usually $C_{L,i} < C_{L,md}$, hence $y < 1$, the angle defined by the arctan is small, and the arctan can be set equal to its argument. This yields a very good approximation of Equation 5.13,

$$R_{h,M} = R_H \mathcal{P}_i \zeta \left(1 - \zeta \frac{y^2}{1+y^2} \right)^{-1} \quad (5.14)$$

For $y \approx 1$ the range is only slightly shorter than for the cruise/climb, but the penalty due to the altitude constraint increases when $C_{L,i} < C_{L,md}$. If the available engine thrust limits the initial cruise altitude appreciably, it is the usual practice to execute intermediate step climbs to increased flight levels, the co-called "*stepped cruise/climb*," in order to approximate the continuous cruise/climb as closely as possible.

Horizontal cruise, constant engine setting (h,es): the decreasing AUW results in an increasing flight speed during the cruise. Formally, the range can be written as follows:

$$R_{h,es} = R_H \mathcal{P}_i \int_{1-\zeta}^1 (\eta/\eta_i) d(W/W_i) \quad (5.15)$$

Due to the increasing speed the overall efficiency increases as well, but an analytical solution is rather complicated. For the special case of constant TSFC a graphical procedure has been proposed by Peckham [19]. No attempt has been made here to derive a general solution, since the following considerations would make such a solution virtually useless.

- ATC requirements and practical flight procedures disfavour the variation in flight speed.
- The present section deals with subcritical speeds, but it is very likely that during the flight the aircraft will enter the drag rise.

Initial conditions: Equations 5.9 and 5.10 show that the maximum range is obtained for initial flight altitude and Mach number such that the initial \mathcal{SR} is maximal. For the horizontal cruise with constant Mach number, however, Equation 5.13 contains not only \mathcal{P}_i but the ratio $y = C_{L,i}/C_{L,md}$ as well. In other words, the mean value of the \mathcal{SR} should be maximized, not the initial value.

Differentiation of Equation 5.13, assuming a *specified Mach number*, yields an optimum altitude defined by

$$y = \frac{1}{\sqrt{1-\zeta}} \quad (5.16)$$

For a *specified altitude* the optimum Mach number is determined by

$$y = \left\{ \frac{2 - \eta_M}{(2 + \eta_M)(1 - \zeta)} \right\}^{1/2} \quad (5.17)$$

These two conditions are incompatible for jet propulsion ($\eta_M > 0$), the same finding of Section 3.1. The aircraft will thus tend to improve its performance by flying faster and higher, until an engine thrust limit is met, which forms the ultimate constraint. The best range performance will then be obtained for an initial lift coefficient determined by

$$y = \frac{1}{\sqrt{(1 + \eta_M)(1 - \zeta)}} \quad (5.18)$$

Contrary to what is usually suggested in the literature this equation shows that for long range flight the optimum initial lift coefficient can be quite close to the minimum drag condition. For example, a fuel fraction of 30% for a turbofan powered airplane, with $\eta_M = 0.60$, yields an optimum $y = 0.945$. The optimum flight speed is then only a few percents above the Minimum Drag Speed.

5.3 Range at High Speeds

Figure 5.1 shows an enlarged sector of Figure 4.3 near the unconstrained maximum of the Range Parameter. The flight condition for maximum \mathcal{SR} is Point A, corresponding to Point A in Figure 4.6. The absolute maximum range will be obtained in a cruise/climb with constant \mathcal{P} for every AUW, resulting in

$$R_{max} = R_H \mathcal{P}_{max} \log(1 - \zeta)^{-1} \quad (5.19)$$

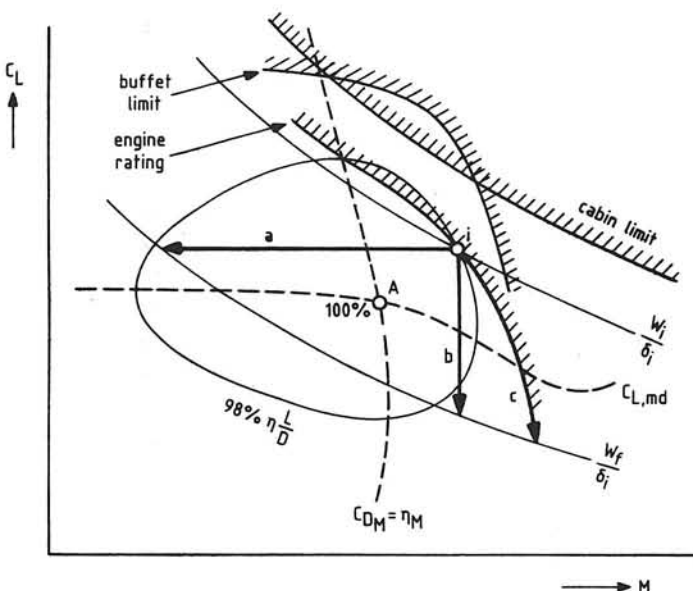


Figure 5.1: Flight schedules for high speed cruising

Although in the present example the available thrust allows the aircraft to fly continuously at this optimum, this procedure is usually not selected in operational practice. For example, *long range cruising* is carried out in a flight condition where the specific range is 98% or 99% of its maximum value. The small fuel penalty is considered acceptable in view of the time saved due to the higher cruise speed. For *short haul flights* a larger fuel penalty can be accepted and the aircraft is flown at the maximum cruise rating of the engines at a lower altitude. These practical flight conditions are referred to as Long Range Cruise (LRC) and High Speed Cruise (HSC) conditions, respectively. Gusty conditions may as well force the pilot to reduce the cruise lift coefficient below its optimum value by flying at a reduced flight level in order to avoid buffeting problems and to improve comfort.

The initial condition of the flight—denoted “i” in Figure 5.1—has been selected so that several flight schedules are possible with only slightly different ranges. In a stepped climb the idealized cruise/climb can be approximated, where the aircraft stays in Point “i”. A horizontal cruise with constant lift coefficient, line “a”, carries the aircraft almost “over the top” of the \mathcal{SR} and yields a good range, as opposed to the low speed case. In spite of this, the speed reduction during the flight is usually objectionable for practical operation. A horizontal cruise with constant Mach number, line “b”, is another schedule “over the top”, which may even be superior to the cruise/climb staying in Point “i”. Cruising with constant engine setting, line “c”, is the only schedule which brings the aircraft to

significantly lower Range Factors because it penetrates the drag rise deeply.

Similar to flying at subcritical speeds the constant altitude and Mach number cruise appears to be preferable. Different from the low speed case, the latter flight schedule does not necessarily have a significant unfavourable effect on the range. Equation 5.13 will therefore be selected² for further use to calculate the fuel load. Again the question is: at what altitude and Mach number should the cruising flight be started? Although for given Mach number P_i is maximum for $C_{D_L} = 1$, hence $y = 1$, the reduction in lift coefficient during the flight brings the optimum theoretically to a higher value. However, the high “optimal initial altitude” may not be achievable in practice due to a thrust limit, a pressure cabin limit or a required buffet margin. For practical performance analysis it is appropriate to select the intersection of the 98% or 99% maximum V/F condition and the cruise thrust limit as the initial flight condition.

²This equation was derived for parabolic drag polars. Since during the flight the Mach number is constant, the drag polar may be different from the low speed case, but it usually remains a parabola.

Chapter 6

Prediction of the Fuel Load

A typical mission profile for an international flight is shown on Figure 6.1. Total fuel is subdivided into

- *block fuel* required to fly the complete mission, including fuel to taxi out before take-off and taxi in after landing, and
- *reserve fuel*, in accordance with the pertinent rules for the operation under consideration.

For the determination of the Take Off Weight (TOW) taxi fuel is not included since the TOW is defined at the runway threshold, before starting the take off. Taxi fuel after landing is usually taken from the reserve fuel, except for multi mission operation. *Mission fuel* includes fuel required for

- take off, acceleration and climb to cruise altitude,
- cruising flight (with or without steps),
- descent, approach and landing,
- manoeuvering.

The AUW of a transport aircraft is subdivided into Operating Empty Weight (OEW), Payload Weight and Fuel Weight. The payload plus fuel load is referred to as the Useful Load (UL). For a given aircraft, the OEW is considered to be independent of the range. The payload is limited (see Figure 6.2) by the Volumetric Payload—determined by the number of seats and volume of the cargo holds—or by the Maximum Zero Fuel Weight (MZFW), a structural limit. In the early design stage maximum payload is determined directly by the design specifications. For short ranges the required mission fuel is determined by the Landing Weight (LW), which in turn depends on the payload.

Figure 6.2 illustrates that the mission fuel versus range is located within an envelope, initially determined by the case of zero payload and by the MZFW, assuming that the latter forms the critical payload limit. The AUW increases with range until it reaches

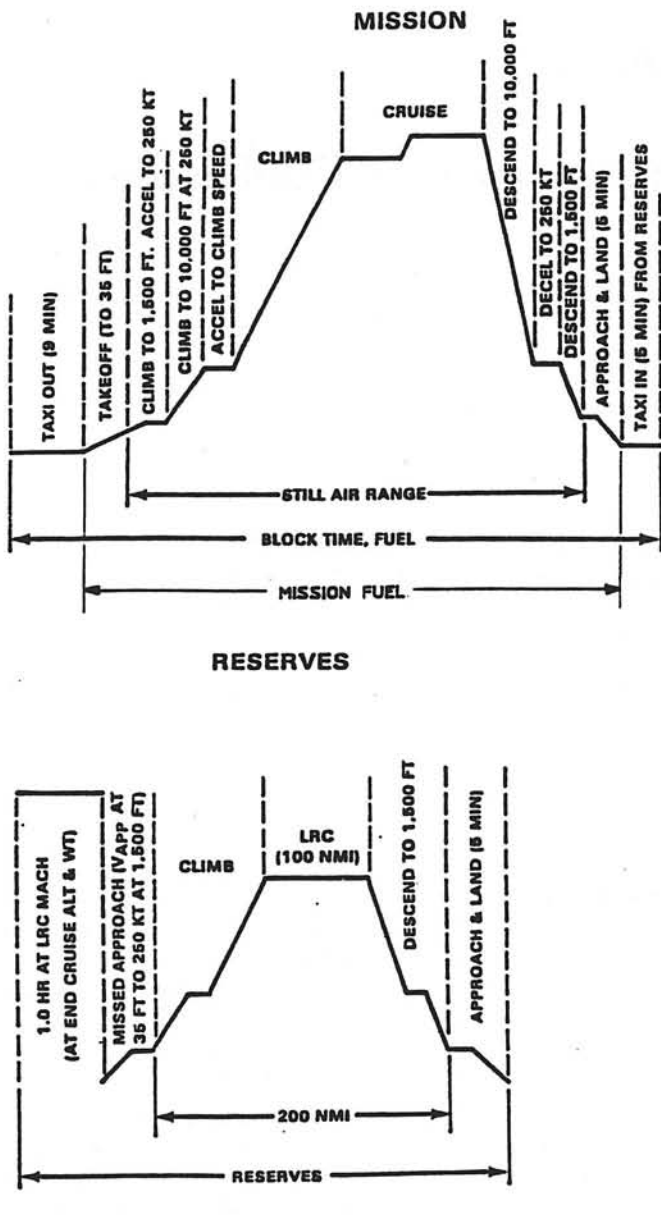


Figure 6.1: A typical flight mission

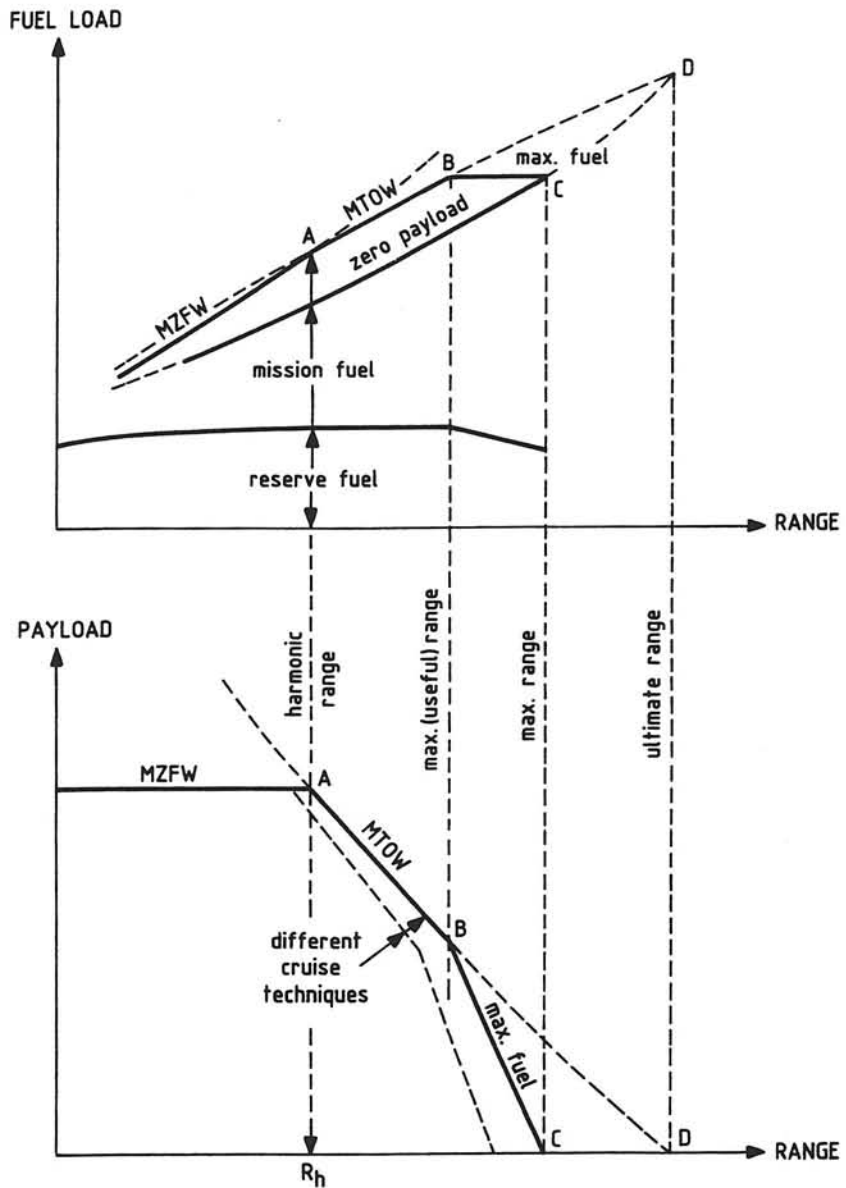


Figure 6.2: Payload and fuel load envelopes versus range

its limit, assumed here as the MTOW. The maximum range with Maximum Payload is referred to as the Nominal or Harmonic Range, Point A in Figure 6.2. For increasing ranges the fuel required is determined by the MTOW, which is independent of the range. The highest payload is than obtained by subtracting the Fuel Weight plus the OEW from the MTOW.

A further increase in range and fuel is limited by the fuel tank capacity corresponding to the maximum useful range: Point B. The maximum range, Point C, is obtained by decreasing the MTOW through progressive payload reduction, since the fuel fraction can be increased only by reducing the initial weight. In the absence of a fuel tank capacity limit the ultimate range¹, Point D, would be reached, where the total fuel load is equal to the MTOW minus the OEW.

The payload versus range and fuel versus range diagrams depend on the cruise technique. In particular there is a considerable difference between Long Range Cruise (LRC) and High Speed Cruise (HSC) techniques; see also Section 5.3. Furthermore there are effects of atmospheric conditions, assumptions with respect to wind, climb and descent flight profiles, reserve fuel policy and various payload configurations of the aircraft, which make it difficult to compare otherwise similar aircraft on their payload versus range diagrams. Nevertheless, it will be shown in the Appendix that these diagrams can provide useful information.

6.1 Mission Fuel

Accurate calculation of the contributions to the fuel load required for various flight segments can only be done when sufficiently detailed data are available in the form of drag polars, engine thrust and fuel flow diagrams, design weights, etc. However, in the conceptual design stage the AUW is to be estimated from elementary information such as the maximum payload, the range, some preliminary engine data and basic aircraft dimensions. In that case it will often be acceptable to estimate the fuel weight fraction W_F/W_{to} on the basis of primarily the cruise fuel requirements. Additional allowances can be given for other flight segments, in particular climb and descent. A major factor to be used as input for such a method will be the range factor $\mathcal{P} = \eta L/D$ at the initial cruise altitude.

A practical procedure to calculate the mission fuel is to determine the amount of fuel required for a *hypothetical cruising flight* over the complete specified (still air) mission range, starting the cruising flight with TOW. An extra amount of fuel ΔW_F is than added to allow for excess fuel consumed during take off, climb to cruise altitude and acceleration to cruise speed, referred to as "lost fuel" [2].

The analysis of range performance has resulted in expressions for the range according to several flight schedules. Recommended expressions are

¹Sometimes referred to as the "Ferry Range", flown for special purposes with extra fuel tanks installed in the fuselage.

- Equation 5.14: subcritical speeds, single parabolic drag polar, for a flight schedule with constant altitude and constant Mach number.
- Equation 5.19: the maximum achievable range for a high speed cruise/climb schedule, a significant result for theoretical work.

The first of these equations is also applicable to high speed cruising. A slightly more refined version is proposed to cover all practical cases by using a “cruise control factor k_R ”. This factor has been developed to offer the possibility to compare different cruise procedures, using the same basic equation for the *cruise fuel load*,

$$\frac{W_{F,cr}}{W_{to}} = \frac{R/R_H}{\mathcal{P}_i + 0.5k_R R/R_H} \quad (6.1)$$

where \mathcal{P}_i denotes the Range Factor $\eta L/D$ at the initial cruise condition, and the cruise control factor is

$$k_R = 1 + \frac{R/R_H}{6\mathcal{P}_i} \quad \text{for a cruise/climb}$$

$$k_R = \left(1 - \frac{R/R_H}{6\mathcal{P}_i}\right) \frac{2y^2}{1+y^2} \quad \text{for horizontal cruise, constant Mach number}$$

For a step/climb k_R will have a value in between these two; a simple assumption $k_R = 1$ will be adequate.

The following advice for the *initial conditions* is based upon the previous analysis.

- For subcritical cruise speeds use Equation 5.18 to find the optimum initial lift coefficient for a horizontal cruise with a thrust constraint. The initial Mach number is then obtained from the equilibrium condition Thrust=Drag, Equation 4.21. For reasons of speed stability it should be above the Minimum Drag Mach number.
- For high speeds the condition for the unconstrained maximum Range Factor should be determined first, as well as the contour of 99% or 98% of this value. The intersection of this curve with the thrust limit is a good initial cruise condition; see also Figure 5.1.

For a more superficial approximation one may simply use $k_R = 1$, and the Range Parameter for LRC is assumed equal to 98% of its maximum value.

The *lost fuel* may be obtained from an energy balance [28],

$$\Delta W_F \eta_{cl} R_H = W_{to} h_{cr} + \frac{W_{to}}{2g} V_{cr}^2 = W_{to} h_{e,cr} \quad (6.2)$$

where η_{cl} denotes the mean value of the overall efficiency during take-off and climb to cruise altitude. Although η_{cl} is dependent on the speed schedule selected for the climb

and on the type of propulsion, it may be assumed equal to a certain fraction of the value during cruising flight. In terms of the energy height at the top of the climb,

$$h_{e,cr} = h_{cr} + \frac{V_{cr}^2}{2g} \quad (6.3)$$

one finds [28]

$$\frac{\Delta W_F}{W_{to}} \approx (1.1 + 0.5\eta_M) \frac{h_{e,cr}}{\eta_{cr} R_H} \quad (6.4)$$

The *additional fuel* to account for manoeuvering [24] amounts to

$$\frac{\Delta W_F}{W_{to}} \approx 0.0025/\eta_{cr} \quad (6.5)$$

Adding these losses to the cruise fuel results in the **mission fuel** for the mission range R_m ,

$$\frac{W_{F,m}}{W_{to}} = \frac{R_m/R_H}{P_i + 0.5k_R R_m/R_H} + \frac{(1.1 + 0.5\eta_M)h_{e,cr}/R_H + 0.0025}{\eta_{cr}} \quad (6.6)$$

In accordance with procedures sometimes adopted in airline evaluations of proposed aircraft the fuel consumed during descent, approach and landing is assumed to be equal to the fuel used during a cruising flight over the same distance. It is thus assumed that a hypothetical cruising flight extension up to the field of destination is made without any further allowances for the actual fuel used, generally a conservative approach.

A further simplification can be made by writing Equation 6.6 as follows:

$$\frac{W_{F,m}}{W_{to}} = \frac{R_{eq}/R_H}{P_i} \quad (6.7)$$

The **equivalent range** R_{eq} is obtained from Equation 6.6

$$R_{eq} = \frac{R_m}{1 + 0.5k_R(R_m/R_H)/P_i} + \{(1.1 + 0.5\eta_M)h_{e,cr} + 0.0025R_H\}(L/D); \quad (6.8)$$

The second term, accounting for the “lost fuel,” amounts to approximately 5% for very long range flights (≈ 12000 km) up to 25% of the first term for relatively short ranges (≈ 1200 km). For every shorter ranges this term will become dominant, but due to its low accuracy a more accurate (numerical) procedure will than be required.

6.2 Reserve and Total Fuel

Reserve fuel will usually include fuel required for

- a diversion flight over a specified distance, including a missed approach and overshoot manoeuvre,

- a holding flight of specified duration at a specified altitude,
- contingency fuel, a certain percentage of the block fuel.
- an extended duration of the flight.

A reserve policy will combine several of these contributions, in accordance with governmental or company rules and dependent on the type of operation. There are important differences in reserve fuel policy between domestic and international flights on the one hand, and between different nations and operators on the other hand. For example, the Association of European Airlines (AEA) specifies

- a 200 nm (370 km) diversion flight for short and medium range aircraft, or a 250 nm (463 km) diversion for long range aircraft,
- 30 minutes holding at 1500 ft (457 m) altitude,
- 5% of the mission fuel for contingency reserve.

For flights in the USA typical reserves are less, for example 130 nm (241 km) diversion and 30 minutes holding at 1500 ft (457 m) altitude. For business aircraft the reserves are in total frequently specified to be equal to a 3/4 hour extension of the cruising flight. Long range international flights may also require an extension of the cruise, for example one hour at LRC flying.

Reserve fuel estimation for preliminary design should be based on a method which allows the user to insert the actual reserve policy for the case under consideration. This results in the selection of several of the following allowances in accordance with the design specification:

1. A *diversion distance* equal to ΔR_{div} flown at the landing weight, expressed as an increase of the mission range,

$$\Delta R = (r \Delta R)_{div} \frac{W_{land}}{W_{to}} \quad (6.9)$$

where the factor r_{div} accounts for the fuel penalty due to the overshoot, and the deterioration in the \mathcal{SR} due to flying at reduced speed and altitude.

2. An allowance for a *holding period* of Δt_{hold} flown at the landing weight, in terms of a mission range increment,

$$\Delta R = (r V \Delta t)_{hold} \frac{W_{land}}{W_{to}} \quad (6.10)$$

where the factor r_{hold} accounts mainly for the reduced powerplant efficiency due to the low altitude and RPM during holding.

3. A *contingency fuel* fraction $\Delta W_{F,ctg}/W_{F,m}$ equal to 0.05 or 0.10.
4. An *extension time* of the cruising flight Δt_{cr} , resulting in an increment of the design range $\Delta R = V_{cr}\Delta t_{cr}$.

The total fuel load is obtained from summation of mission fuel (Equation 6.6) and the various reserve fuel allowances discussed in the previous paragraph. It is appropriate here to introduce the **equivalent all-out range** \mathcal{R}_i for the case that diversion, holding and contingency fuel are specified,

$$\mathcal{R} = R_{eq} \left\{ 1 + \frac{\Delta W_{F,ctg}}{W_{F,m}} \right\} + \{(r V \Delta t)_{hold} + (r \Delta R)_{div}\} \frac{W_{land}}{W_{to}} + (V \Delta t)_{cr} \quad (6.11)$$

The holding speed is generally about 50% of the cruising speed, while $W_{land}/W_{to} = 1 - W_{F,m}/W_{to}$. The penalty factors r_{hold} and r_{div} may require a rather complex calculation procedure, but the following rule of the thumb is proposed as an alternative:

$$r_{hold} = r_{div} \approx 1.10 + 0.5\eta_M \quad (6.12)$$

If the reserves are specified as a continued duration of the cruising flight, the equivalent all-out range is simply

$$\mathcal{R} = R_{eq} \left\{ 1 + \frac{\Delta t_{cr}}{t_{cr}} \right\} \quad (6.13)$$

Finally the total fuel fraction is obtained from

$$\frac{W_F}{W_{to}} = \frac{\mathcal{R}/R_H}{\mathcal{P}_i} = \frac{\mathcal{R}/R_H}{(\eta L/D)_i} \quad (6.14)$$

The advantage of these analytical equations is that they provide a closed-form, non-iterative, and therefore computationally very efficient method for calculating the total fuel load fraction.

Chapter 7

Summary of Results

In spite of the large amount of literature on optimum range performance there is still no undisputed generalized approach. The present report forms a basis for such a solution. Analytical criteria are presented for the unconstrained optimum of the Specific Range, which—in the case of tubofan powered aircraft—occurs at high subsonic speeds. For subcritical speeds only constrained optima exist. All criteria are given in relation to the powerplant overall efficiency and its derivative with respect to the Mach number and engine rating. They apply to any presently existing gas turbine based propulsion system for subsonic aircraft. Most criteria found in the literature are special cases of the general theory presented in the present report.

Logarithmic derivates have proved to be very useful for the present analysis to derive optimum cruise conditions; they are defined as follows:

- $C_{D_L} = \partial \log C_D / \partial \log C_L$
- $C_{D_M} = \partial \log C_D / \partial \log M$
- $\eta_M = \partial \log \eta / \partial \log M$

The present approach obviates the classical assumptions made in many previous publications on cruise performance: compressibility effects are absent, the drag polar is parabolic, the overall powerplant efficiency or TSFC is constant.

The range parameter is a non-dimensional generalized cruise performance index,

$$\mathcal{P} = \eta L/D$$

The Specific Range \mathcal{SR} appears to be proportional to this parameter, according to Equation 4.4,

$$\frac{V}{F} = \frac{R_H}{W} \mathcal{P}$$

The combined aerodynamic/propulsive quality of aircraft with widely different AUW can be compared on the basis of this Range Parameter. For a given aircraft/engine combination \mathcal{P} is a unique function of the lift coefficient and the Mach number only, and it appears advantageous to represent it in a C_L versus M diagram; see for example Figure 4.3.

For subcritical speeds where a single drag polar is used—e.g. for propeller aircraft—an unconstrained optimum is possible only for $\eta_M = 0$, hence constant overall efficiency or an efficiency which reaches a maximum value. In the latter case both the lift/drag ratio and the overall efficiency can have a maximum value at the same altitude and speed, provided the altitude is chosen appropriately, according to Equation 4.13. For turbofan engines $\eta_M > 0$, and there will only be a constrained optimum,

- *altitude constraint:* $C_{D_L} = 1 - \eta_M/2$ or, in the case of a parabolic drag polar:

$$C_L = C_{L,md} \sqrt{\frac{2 - \eta_M}{2 + \eta_M}}$$

- *thrust constraint:* $C_{D_L} = 2/(2 + \eta_M)$ or, in the case of a parabolic drag polar:

$$C_L = C_{L,md} \frac{1}{\sqrt{1 + \eta_M}}$$

The latter is the most significant of the two constraints. For $\eta_M = 1$ these results are in accordance with classical criteria for constant TSFC.

Unconstrained optima for high speeds: the drag coefficient, the lift/drag ratio and the range parameter are essentially a function of the lift coefficient and the Mach number. Optimum conditions have to be defined in terms of both C_L and M , as opposed to the case of a single drag polar. Conditions for the unconstrained optimum are

- $C_{D_L} = 1 \rightarrow \partial C_D / \partial C_L = 1 \rightarrow C_L = C_{L,md}$
- $C_{D_M} = \eta_M \rightarrow \partial C_D / \partial M = \eta_M C_D / M$

defining a flight condition in the drag rise, slightly below the drag divergence Mach number.

Reference is made to Figure 7.1, depicting the following unconstrained optima:

- *propeller aircraft* with constant overall efficiency: $\eta_M = 0$ defining $(L/D)_{max}$ at Point A_1 .
- *idealized jet propulsion* with constant TSFC: $\eta_M = 1$ resulting in $\partial C_D / \partial M = C_D / M$, hence $(ML/D)_{max}$, Point A_2 . This curve in Figure 7.1 can also be found directly from the drag polars; see Figure 2.3.

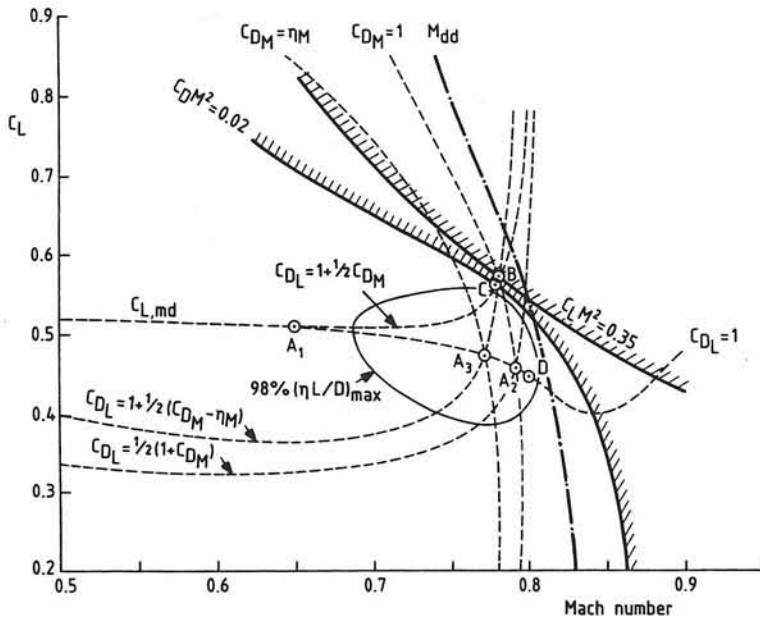


Figure 7.1: Overview of the partial and constrained optima

- *turbofan propulsion*: $0 < \eta_M < 1$, the maximum for the \mathcal{SR} at Point A_3 . Typical values for η_M are between 0.4 and 0.8; see Figure 4.4.

Although Point A_3 is theoretically the condition for maximum Specific Range it is usual to fly long distances at a somewhat higher Mach number, thereby accepting one or two percent increase in fuel consumption: the Long Range Cruise condition, LRC.

Constrained optima for high speed flight: operational considerations—e.g. Air Traffic Control or a cabin pressure limit—may force the aircraft to fly at a specified altitude, imposing a constraint on $C_L M^2$. In combination with the general requirements for maximizing \mathcal{P} defined by Equation 4.11 this constraint is: $C_{D_L} = 1 + (C_{D_M} - \eta_M)/2$. In Figure 7.1 this equation must be intersected with the specified value of $C_L M^2$, resulting in the optimum Point B .

A similar constraint due to the engine thrust limit on T/δ , or on $C_D M^2$, results in the following condition: $C_{D_L} = (2 + C_{D_M})/(2 + \eta_M)$, which defines the optimum Point C after intersection with the specified value of $C_D M^2$.

Other factors affecting the optimum may be associated with:

- the occurrence of *multiple optima*, see Section 4.2,

- *refinements in the analysis* associated with realistic engine rating limits and installation effects, see Section 4.4,
- operational and/or economic considerations which may result in *off-optimum flight conditions*.

For example, Point D ($M = 0.8$, $C_L = 0.45$) in Figure 7.1 could be a suitable initial value for long range cruising, since excursions to higher or lower lift coefficients will not degrade the \mathcal{SR} by more than a few percent of its maximum value. If for operational reasons the cruise Mach number has to be reduced, the \mathcal{SR} is in fact slightly improved. Final selection of the High Speed Cruise condition (HSC) will be based on economic considerations which are outside the scope of this report.

Range in cruising flight is obtained from integration of the Specific Range. Several flight schedules have been used for deriving the integrated range in Section 5.2. The cruise/climb schedule is often used in theoretical work but the constant altitude and Mach number flight is more practical from the operational point of view. An accurate approximation for the range is

$$R = R_H \mathcal{P}_i \frac{\zeta}{1 - 0.5k_R \zeta} \quad (7.1)$$

where ζ denotes the fuel fraction W_F/W_i and k_R is defined by Equation 6.1 for several flight schedules. Usually k_R is close to one, but lower values apply to constrained flight conditions.

Calculation of the Fuel Load: using the approach presented in Sections 6.1 and 6.2 the mission and reserve fuel loads can be computed by means of closed form analytical expressions, avoiding the usual labourious iterative procedure. The essential input required is the initial cruise Range Parameter \mathcal{P}_i , which can be selected on the basis of the described optimization process. If detailed data of the design are lacking, the Appendix proposes a method for obtaining this factor from existing aircraft data, using an available payload versus range diagram.

Appendix A

Statistical Derivation of the Range Parameter

Section 4.2 was devoted to the analysis of flight conditions resulting in the maximum value of the Range Parameter. Unconstrained as well as constrained maxima have been treated and the availability of drag polars and some basic engine data will suffice to calculate the (initial) Range Parameter required for the mission fuel computation. In some cases, however, it may be useful to estimate \mathcal{P}_i from statistical data for the Range Parameter of existing aircraft derived from published payload versus range diagrams. The most significant part of this diagram, see Figure A.1, is sector AB, corresponding to take off with MTOW. At point A, referred to as the Harmonic or Nominal Range R_h , the slope of this line is equal to minus the increase in cruise fuel required for a small range increment, which is found from differentiation of Equation 5.14, for $y = 1$,

$$d(R_h/R_H) = \mathcal{P}_i \frac{d(W_F/W_{to})}{(1 - 0.5W_F/W_{to})^2} \quad (\text{A.1})$$

Substitution of the fuel fraction according to Equation 6.1 with $k_R = 1$ yields a quadratic equation in \mathcal{P} , for which an approximate solution is

$$\mathcal{P}_i = \sqrt{\Phi(\Phi - 2R_h/R_H)} \quad (\text{A.2})$$

where the normalized slope of the payload versus range diagram has been introduced,

$$\Phi \stackrel{\text{def}}{=} \frac{d(R/R_H)}{d(W_F/W_{to})} \approx \frac{W_{to}}{R_H} \frac{\Delta R}{-\Delta W_p} \quad \text{for } R = R_h \quad (\text{A.3})$$

The identity $\Delta W_F = -\Delta W_p$ is strictly only valid when the reserve fuel is a constant fraction of the MTOW; since this is not exactly true a prediction error of plus or minus five percent may be introduced. The (negative) slope of the range versus the payload ($\Delta R/\Delta W_p$) can be measured in the payload versus range diagram; see Figure A.1. Although Equation A.2 has been derived for flight at constant altitude and Mach number, it is an equally good approximation when the cruise fuel is derived from the Bréguet range equation.

PAYOUT

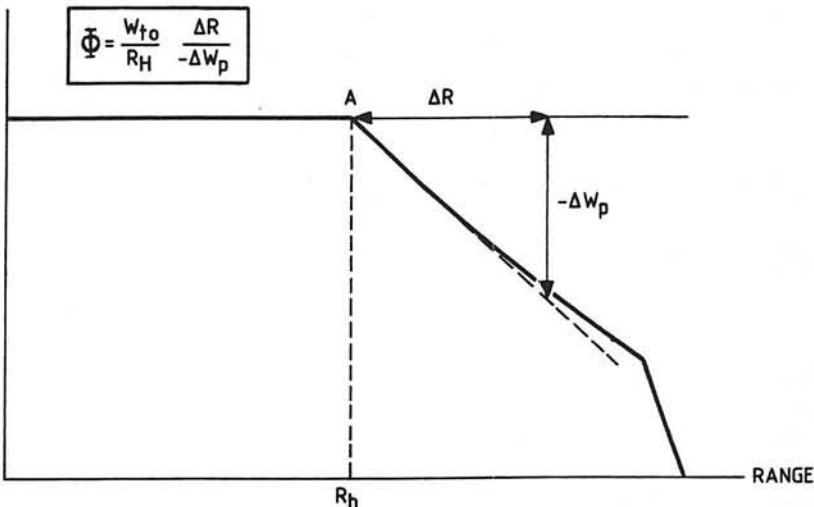


Figure A.1: Derivation of \mathcal{P}_i from a payload versus range diagram

The method derived in this paragraph has been used to obtain a mean value of the Range Parameter for a number of existing aircraft, for which a payload versus range diagram was available to the author. The result is found in Tables 1 and 2¹, from which the following observations can be made:

1. Large long range turbofan powered transport aircraft achieve the highest range factors: presently (1995) about 6.5 to 7.0 for modern, very long range transports for LRC conditions, and about 10% less for HSC.
2. The Range Factor is affected by the size of the aircraft: large aircraft have higher values than small ones.
3. Short range aircraft are considerably less efficient in fuel usage due to their low range factor. This is a result mainly of their flight taking place at lower altitudes and relatively short cruise sectors, contributing to a reduced mean value of the \mathcal{SR} for the overall flight.
4. In spite of the high propulsive efficiency of propellers the most fuel efficient propeller aircraft reach their limit at about 4.5 for LRC conditions, and 15-20% below this value for HSC.

¹Due to differences in reserve fuel policy, aircraft should not be compared on the basis of only these derived data.

5. For several aircraft categories the effect of improvements in the state-of-the-art can be clearly seen. For example, for the Boeing 707/320 which was designed during the fifties, the range parameter was about 4.5 for LRC, while the more recent Boeing 757 and 767 achieve 5.2 and 5.7, respectively. The present day, very long range transport aircraft establish the practical limit of current state-of-the art: a range factor of about 6.5 to 7, complying with a lift/drag ratio of about 20 and an overall powerplant efficiency near to 35%.

Aircraft type	MTOW (lb)	R_h (nm)	$\Delta W_F/\Delta R$ (lb/nm)	$(\eta L/D);$ (—)	Remarks
Airbus A 300-B2	302,030	860	25.82	4.55	HSC: 3.56
Airbus A 310-220	291,000	1,245	21.48	5.16	
Airbus A 320-200	158,510	1,265	11.80	5.10	A 320-100: 4.60
Airbus A 330	467,400	3,233	23.76	6.78	GE CF-6-81 eng.
Airbus A 340-200	566,600	5,475	25.54	6.65	
Airbus A 340-300	566,600	4,965	26.66	6.57	
Boeing 707-320	312,000	4,280	19.61	4.55	LRC
Boeing 727-200	169,000	948	15.13	4.29	
Boeing 737-300	124,500	952	10.37	4.64	
Boeing 747-300	833,000	4,750	48.39	4.85	
Boeing 747-400	850,000	5,600	43.97	5.28	
Boeing 757	220,000	1,100	16.41	5.16	
Boeing 767-200	335,000	2,930	19.75	5.78	
Boeing 777	535,000	3,100	26.47	7.12	
Br.Aerospace 146-100	84,000	925	9.65	3.26	
Br.Aerospace 146-200	93,000	1,175	11.83	2.77	
BAC 1-11-400	88,500	980	8.84	3.78	99% max.range
BAC 1-11-500	99,650	880	10.49	3.62	
Canadair Challenger	43,100	2,557	3.45	4.04	CF-34, LRC M=0.74
Fokker F-28/2000	65,000	440	12.71	1.96	HSC
Fokker 100	91,500	780	9.08	3.90	LRC
Lockheed L-1011/100	426,000	2,500	28.92	5.05	HSC: 4.96
Lockheed L-1011/500	496,000	3,660	30.03	5.21	
McD.Douglas DC-8/61	325,000	2,550	25.40	4.18	
McD.Douglas DC-8/63	350,000	3,400	23.32	4.68	
McD.Douglas DC-9/50	121,000	765	11.53	4.09	
McD.Douglas DC-9/80	140,000	820	14.07	3.83	
McD.Douglas DC-10/10	440,000	2,330	30.07	5.09	
McD.Douglas DC-10/30	572,000	4,167	34.98	4.83	
VFW-614	44,000	658	7.81	2.08	

Table 1: The derived Range Parameter for turbofan powered aircraft

Aircraft type	MTOW (lb)	R_h (nm)	$-\Delta W_F/\Delta R$ (lb/nm)	$(\eta L/D)_i$ (—)	Remarks
ATR-42/100	32,440	776	3.00	4.22	HSC: 3.58
ATR-42/200	34,280	910	2.97	4.46	HSC: 3.82
ATR-72	44,070	0	4.47	4.15	LRC
B.Aerosp. ATP	49,500	560	4.95	3.97	LRC
B.Aerosp. Jetstream	15,322	600	2.11	2.93	HSC: 2.60
D.H.Canada Dash-7	44,000	678	5.79	2.90	
D.H.Canada Dash-8	34,500	550	3.33	4.12	HSC: 3.74
Dornier Do-228/200	12,500	580	2.33	2.00	
Embraer Brasilia	24,250	260	2.98	3.32	
Fokker F-27-Mk500	45,900	600	5.64	3.16	LRC
Fokker 50 Basic	41,865	100	3.98	4.39	HSC: 3.47
Fokker 50 incr.MTOW	45,900	900	4.26	4.14	LRC
Hawker Siddeley 748	46,500	755	4.95	3.42	
Piaggio P-180	10,150	800	1.03	3.93	320 kts
SAAB-Fairchild 340	27,275	300	3.35	3.30	LRC @ 25 000 ft
Fairchild Metro III	16,000	760	1.79	3.43	

Table 2: The derived Range Parameter for turboprop aircraft

Bibliography

- [1] Anonymus, "Non-dimensional Graphical Method for the Analysis of Measurements of Steady Level Speed, Range and Endurance: Aircraft with Turbo-jet and Turbo-fan Engines," ESDU Item No. 70022, October 1973, Performance Volume 10.
- [2] Anonymus, "Approximate Methods for Estimation of Cruise Range and Endurance: Aeroplanes with Turbo-jet and Turbo-fan Engines," ESDU Item No. 73019, May 1982, Performance Volume 6.
- [3] Anonymus, "Introduction to Estimation of Range and Endurance," ESDU Item No. 73018, October 1980, Performance Volume 6.
- [4] Ashkenas, I.L., "Range Performance of Turbojet Airplanes," *Journal of the Aeronautical Sciences*, Vol. 15, Feb. 1948, pp. 97-101.
- [5] Backhaus, G., "Grundbeziehungen für den Entwurf optimaler Verkehrsflugzeuge," *Jahrbuch der WGLR*, 1958, pp. 201-213.
- [6] Bert, C.W., "Prediction of Range and Endurance of Jet Aircraft at Constant Altitude," *Journal of Aircraft*, Vol. 18, 1981, pp. 890-892.
- [7] Dommasch, D.O., Sherby, S.S., and Connolly, T.F., *Airplane Aerodynamics*, Pitman, New York, 1957, pp. 286-287.
- [8] Edwards, A.D., "Performance Estimation of Civil Jet Aircraft," *Aircraft Engineering*, Vol. 22, No. 254, April 1950, pp. 94-99.
- [9] Hale, F.J., "Best-Range Flight Conditions for Cruise-Climb Flight of a Jet Aircraft," NASA Conference Proceedings No 2001, Vol. 4, 1976, pp. 1713-1719.
- [10] Hale, F.J. and Steiger, A.R., "Effects of Wind on Aircraft Performance," *Journal of Aircraft*, Vol. 16, June 1979, pp. 382-387.
- [11] Jonas, J., "Jet Airplane Range Considerations," *Journal of the Aeronautical Sciences*, Vol. 14, Feb. 1947, pp. 124-128.
- [12] Mair, W.A. and Birdsall, D.L., *Aircraft Performance*, Cambridge Aerospace Series, Cambridge University Press 1992, ISBN 0-521-36264-4.

- [13] Miller, L.E., "Optimal Cruise Performance," *Journal of Aircraft*, Vol. 30, No. 3, May-June 1993, pp. 403-405.
- [14] Martinez-Val, R. and Pérez, E., "Optimum Cruise Lift Coefficient for Constant Altitude Constraint in Initial Design of Aircraft," *Journal of Aircraft*, Vol. 29, No. 4, 1992, pp. 712-714.
- [15] Martinez-Val, R. and Pérez, E., "Extended Range Operations of Two and Three Turbofan Engined Airplanes," *Journal of Aircraft*, Vol. 30, No. 3, May-June 1993, pp. 382-386.
- [16] Menon, P.K.A., "A Study of Aircraft Cruise," AIAA Paper No. 86-2286 (AIAA Conference Proceedings CP-8687, 1986).
- [17] Miele, A., *Flight Mechanics*, Volume 1: Theory of Flight Paths, Addison Wesley Publishing Inc., Reading, Massachusetts, 1962.
- [18] Page, R.K., "Performance Calculation for Jet-Propelled Aircraft," *Journal of the Royal Aeronautical Society*, Vol. 51, 1947, pp. 440-450.
- [19] Peckham, D.H., "Range Performance in Cruising Flight," Royal Aircraft Establishment Technical Report 73164, March 1974.
- [20] Perkins, C.D. and Hage, R.E., *Airplane Performance, Stability and Control*, Wiley, New York, 1949, pp. 183-194.
- [21] Ruijgrok, G.J., *Elements of Airplane Performance*, Delft University Press, 1990, ISBN 90-6275-608-5.
- [22] Sachs, G. and Christodoulou, T., "Reducing Fuel Consumption of Subsonic Aircraft by Optimal Cyclic Cruise," *Journal of Aircraft*, Vol. 24, 1987, pp. 616-622.
- [23] Schairer, G.S. and Olason, M.L., "Some Performance Considerations of a Jet Transport Airplane," First Turbine Powered Air Transportation Meeting, Institute of the Aeronautical Sciences, Seattle, Washington, August 9-11, 1954.
- [24] Shevell, R.S., *Fundamentals of Flight*, Prentice-Hall, 1983, ISBN 0-13-339093-4.
- [25] Torenbeek, E., "Fundamentals of Conceptual Design Optimization of Subsonic Transport Aircraft," Dept. of Aerospace Engineering, Delft University of Technology, Report LR-292, 1980 (Abstract in STAR N81- 13951).
- [26] Torenbeek, E., "Some Fundamental Aspects of Transport Aircraft Conceptual Design," AGARD Conference Proceedings, No. 280, Paper 5, 1979.
- [27] Torenbeek, E. and Wittenberg, H., "Generalized Maximum Specific Range Performance," *Journal of Aircraft*, Vol. 20, No. 7, July 1983, pp. 617-622.

- [28] Torenbeek, E., "The Initial Calculation of Range and Mission Fuel during Conceptual Design," Dept. of Aerospace Engineering, Delft University of Technology, Report LR-525, 1987.
- [29] Visser, H.G., "Terminal Area Traffic Management," *Progress in Aerospace Sciences*, Vol. 28, pp. 323-368, 1991.

Series 01: Aerodynamics

01. F. Motallebi, 'Prediction of Mean Flow Data for Adiabatic 2-D Compressible Turbulent Boundary Layers'
1997 / VI + 90 pages / ISBN 90-407-1564-5
02. P.E. Skåre, 'Flow Measurements for an Afterbody in a Vertical Wind Tunnel'
1997 / XIV + 98 pages / ISBN 90-407-1565-3
03. B.W. van Oudheusden, 'Investigation of Large-Amplitude 1-DOF Rotational Galloping'
1998 / IV + 100 pages / ISBN 90-407-1566-1
04. E.M. Houtman / W.J. Bannink / B.H. Timmerman, 'Experimental and Computational Study of a Blunt Cylinder-Flare Model in High Supersonic Flow'
1998 / VIII + 40 pages / ISBN 90-407-1567-X
05. G.J.D. Zondervan, 'A Review of Propeller Modelling Techniques Based on Euler Methods'
1998 / IV + 84 pages / ISBN 90-407-1568-8
06. M.J. Tummers / D.M. Passchier, 'Spectral Analysis of Individual Realization LDA Data'
1998 / VIII + 36 pages / ISBN 90-407-1569-6
07. P.J.J. Moeleker, 'Linear Temporal Stability Analysis'
1998 / VI + 74 pages / ISBN 90-407-1570-X
08. B.W. van Oudheusden, 'Galloping Behaviour of an Aeroelastic Oscillator with Two Degrees of Freedom'
1998 / IV + 128 pages / ISBN 90-407-1571-8
09. R. Mayer, 'Orientation on Quantitative IR-thermografy in Wall-shear Stress Measurements'
1998 / XII + 108 pages / ISBN 90-407-1572-6
10. K.J.A. Westin / R.A.W.M. Henkes, 'Prediction of Bypass Transition with Differential Reynolds Stress Models'
1998 / VI + 78 pages / ISBN 90-407-1573-4
11. J.L.M. Nijholt, 'Design of a Michelson Interferometer for Quantitative Refraction Index Profile Measurements'
1998 / 60 pages / ISBN 90-407-1574-2
12. R.A.W.M. Henkes / J.L. van Ingen, 'Overview of Stability and Transition in External Aerodynamics'
1998 / IV + 48 pages / ISBN 90-407-1575-0
13. R.A.W.M. Henkes, 'Overview of Turbulence Models for External Aerodynamics'
1998 / IV + 40 pages / ISBN 90-407-1576-9

Series 02: Flight Mechanics

01. E. Obert, 'A Method for the Determination of the Effect of Propeller Slip-stream on a Static Longitudinal Stability and Control of Multi-engined Aircraft'
1997 / IV + 276 pages / ISBN 90-407-1577-7
02. C. Bill / F. van Dalen / A. Rothwell, 'Aircraft Design and Analysis System (ADAS)'
1997 / X + 222 pages / ISBN 90-407-1578-5
03. E. Torenbeek, 'Optimum Cruise Performance of Subsonic Transport Aircraft'
1998 / X + 66 pages / ISBN 90-407-1579-3

Series 03: Control and Simulation

01. J.C. Gibson, 'The Definition, Understanding and Design of Aircraft Handling Qualities'
1997 / X + 162 pages / ISBN 90-407-1580-7
02. E.A. Lomonova, 'A System Look at Electromechanical Actuation for Primary Flight Control'
1997 / XIV + 110 pages / ISBN 90-407-1581-5
03. C.A.A.M. van der Linden, 'DASMAT-Delft University Aircraft Simulation Model and Analysis Tool. A Matlab/Simulink Environment for Flight Dynamics and Control Analysis'
1998 / XII + 220 pages / ISBN 90-407-1582-3

Series 05: Aerospace Structures and Computational Mechanics

01. A.J. van Eekelen, 'Review and Selection of Methods for Structural Reliability Analysis'
1997 / XIV + 50 pages / ISBN 90-407-1583-1
02. M.E. Heerschap, 'User's Manual for the Computer Program Cufus. Quick Design Procedure for a CUt-out in a FUSelage version 1.0'
1997 / VIII + 144 pages / ISBN 90-407-1584-X
03. C. Wohlever, 'A Preliminary Evaluation of the B2000 Nonlinear Shell Element Q8N.SM'
1998 / IV + 44 pages / ISBN 90-407-1585-8
04. L. Gunawan, 'Imperfections Measurements of a Perfect Shell with Specially Designed Equipment (UNIVIMP)
1998 / VIII + 52 pages / ISBN 90-407-1586-6

Series 07: Aerospace Materials

01. A. Vašek / J. Schijve, 'Residual Strength of Cracked 7075 T6 Al-alloy Sheets under High Loading Rates'
1997 / VI + 70 pages / ISBN 90-407-1587-4
02. I. Kunes, 'FEM Modelling of Elastoplastic Stress and Strain Field in Centre-cracked Plate'
1997 / IV + 32 pages / ISBN 90-407-1588-2
03. K. Verolme, 'The Initial Buckling Behavior of Flat and Curved Fiber Metal Laminate Panels'
1998 / VIII + 60 pages / ISBN 90-407-1589-0
04. P.W.C. Provó Kluit, 'A New Method of Impregnating PEI Sheets for the *In-Situ* Foaming of Sandwiches'
1998 / IV + 28 pages / ISBN 90-407-1590-4
05. A. Vlot / T. Soerjanto / I. Yeri / J.A. Schelling, 'Residual Thermal Stresses around Bonded Fibre Metal Laminate Repair Patches on an Aircraft Fuselage'
1998 / IV + 24 pages / ISBN 90-407-1591-2
06. A. Vlot, 'High Strain Rate Tests on Fibre Metal Laminates'
1998 / IV + 44 pages / ISBN 90-407-1592-0
07. S. Fawaz, 'Application of the Virtual Crack Closure Technique to Calculate Stress Intensity Factors for Through Cracks with an Oblique Elliptical Crack Front'
1998 / VIII + 56 pages / ISBN 90-407-1593-9
08. J. Schijve, 'Fatigue Specimens for Sheet and Plate Material'
1998 / VI + 18 pages / ISBN 90-407-1594-7

Series 08: Astrodynamics and Satellite Systems

01. E. Mooij, 'The Motion of a Vehicle in a Planetary Atmosphere'
1997 / XVI + 156 pages / ISBN 90-407-1595-5
02. G.A. Bartels, 'GPS-Antenna Phase Center Measurements Performed in an Anechoic Chamber'
1997 / X + 70 pages / ISBN 90-407-1596-3
03. E. Mooij, 'Linear Quadratic Regulator Design for an Unpowered, Winged Re-entry Vehicle'
1998 / X + 154 pages / ISBN 90-407-1597-1





3021896

A unified analytical treatment of the cruise performance of subsonic transport aircraft is derived, valid for arbitrary gas turbine powerplant installations: turboprop, turbojet and turbofan powered aircraft. Different from the classical treatment the present report takes into account compressibility effects on the aerodynamic characteristics. Analytical criteria are derived for optimum cruise lift coefficient and Mach number, without and with constraints on the altitude and/or the engine rating. A simple alternative to the Bréquet range equation is presented which applies to aircraft cruising at constant altitude and a high Mach number. A practical non-iterative procedure for calculating the mission and reserve fuel loads in the conceptual design stage is proposed as a conclusion of this report.

ISBN 90-407-1579-3



9 799040 715791

